The National Centre for Environmental Data and Surveillance

Development and Testing of Suspended Solids Algorithms Case Study 2

ENVIRONMENT AGENCY

EXECUTIVE SUMMARY

Accurate visualisation of suspended solids concentration gradients using aerial surveillance provides the only realistic means of estimating suspended solids distribution over the coastal zone. This has a clear use for the determination of the fate of pollutants in the coastal zone and for assessing areas prone to flooding.

The subject has been extensively investigated by remote surveillance specialists in the UK and overseas, with a range of algorithms being developed to calibrate aerial imagery for suspended solids concentration.

This study is the most intensive known application of established techniques to aerial imagery collected in coastal waters of England and Wales, and the key findings were:
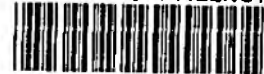
- The development of algorithms to calibrate CASI imagery for suspended solids can allow estimation of suspended solids to a similar accuracy as present boat continuous techniques and allow the visualisation of suspended solids concentrations over a wide spatial scale.

- The algorithm developed for the Bristol Channel site using continuous transmission data as a calibration aid proved to be portable to data collected later in the year. Algorithms for the Norfolk Coast, however, proved not to be portable. This was considered to be due to a lack of suitable continuous transmission data from the survey vessel.

- The algorithms were found to be site specific and could not be used to calibrate CASI data from a different site. However, the portability of algorithms to data from a different date means that a suite of algorithms could be developed for different sections of the coastline with similar morphologies. This would then remove the requirement for costly boat calibration data.

- Present state of knowledge techniques to enhance calibration portability proved to be unhelpful.

The following recommendations are made for the use of such techniques for marine monitoring:

- A suite of algorithms should be developed to calibrate CASI imagery for differing areas of the coastline, based on the empirical algorithm development explored in this case study.

- Innovative techniques from other spectroscopy applications (eg. chemometric techniques) should be investigated in order to improve the portability of the algorithms.

- Underway transmission data should always be collected when relating CASI imagery to suspended solids concentration.

CONTENTS

LIST OF FIGURES

LIST OF TABLES

1. BACKGROUND

1.1 The measurement of suspended solids concentration in coastal waters is important as it provides information on the transfer of major pollutants and their deposition within estuaries and the coastal zone. Accurate spatial measurements of the dynamics and characteristics of sediments will provide the essential information necessary to determine the fate of these pollutants and suggest how problems associated with their build up may be assessed.

1.2 An understanding of the sediment transport characteristics of a region is key in any investigation of erosion and accretion, which is important in the understanding of flood dynamics and prediction. This provides information to assist the Environment Agency in preventing the occurrence of flooding, a requirement set down under the Land Drainage Act (1991) and the Water Resources Act (1991).

1.3 Laboratory spot samples ae not appropriate for the spatial determination of suspended sediment concentration because of the great range in concentrations and the high rate of change in the coastal zone. Continuous track transmissometers increase the spatial sampling capability, but are still inadequate to describe changes across the entire coastal zone.

1.4 Calibration of aerial imagery has been investigated as a means of visualising suspended solids concentration over the entire coastal zone. A range of algorithms have been developed by a number of workers, which usually rely on the variation in the ratio of two wavelengths with suspended solids concentration. Techniques have been developed to remove the effects of light scatter by the atmosphere.

1.5 The purpose of this investigation was to image three coastal areas on at least two occasions and use current best available techniques to investigate the use of CASI imagery to estimate suspended solids concentration. The portability of algorithms both between sites and across seasons will be investigated. This will enable a decision to be made on the potential for routine use of such algorithms for the estimation of suspended solids concentration as part of a marine monitoring strategy.

2. PREVIOUS WORK

2.1 Previous work both by the Environment Agency and by research bodies, has shown that suspended solids concentrations in tidal waters are highly variable, and as such collection of representative samples over wide spatial scales is impractical. Remote sensing methods offer the advantage of collection of synoptic measurements over large areas. However, accurate calibration of the remote sensing signal for suspended solids is necessary to make the data useful.

2.2 Suspended solids within the water column enhance reflected sunlight to the remote sensor across the visible wavelengths. This is most marked in the red and near infra-

1

red wavelengths where reflection by the water column itself is very low.

2.3 The majority of estimates of suspended solids from satellite sensors have been made with the Landsat Multispectral Scanner (MSS). For example, Klemas et al. (1973) found a correlation between suspended solids concentration and the reflectance at 600 -700 nm. Munday and Alfoldi (1979) found that the Landsat radiance correlated best with the logarithm of suspended solids concentration. Ritchie et al. (1990) found that Landsat Thematic Mapper (TM) was useful for the estimation of suspended solids, although its finer spatial resolution makes it more suitable for near shore studies. Stumpf and Pennock (1989) used the red and near infra-red channels of the Advanced Very High Resolution Radiometer (AVHRR) to estimate the suspended solids loading of estuaries at a 1 km resolution.

2.4 In coastal waters, oceanographic phenomena are often of such as scale as to preclude measurement by satellite sensors. Features tend to be smaller than the typical 1 km pixel size of the AVHRR and CZCS sensors. The finer resolution of the Landsat MSS and TM makes this more suitable for coastal scale processes, but the repeat time of overpasses means that when combined with the cloudy conditions often experienced in the UK, only a very few overpasses are available over any particular location, with no control on tidal state at the time of acquisition.

2.5 Collection of data from airborne systems overcomes many of these problems. Aircraft sensors may be flown at low altitude allowing collection of data at a finer spatial resolution. Moreover, these platforms are temporally more flexible, with the ability to collect data at specific tidal sites, to coincide with both good weather conditions and accompanying shipborne studies.

2.6 Algorithms such as those used for satellite sensors have been applied to data from aircraft. Collins and Pattiaratchi (1984) used multiple regression techniques to calibrate Daedalus Airborne Thematic Mapper (ATM) data of the Bristol Channel. Rimmer et al. (1987) used both linear and multiple regression to estimate suspended solids from ATM data in the same region. Mitchelson et al. (1986) established the need for two algorithms to be used dependent on the suspended solids concentration in their work on the Irish Sea.

2.7 The majority of the above algorithms are empirically derived from a combination of remotely sensed measurements and in-situ data. Curran et al. (1987), however, found difficulty in inverting the empirically derived relationships, resulting in errors of 343-394% when calculating suspended solids concentration from the remotely sensed signal.

2.8 Brown and Simpson (1990) concluded that estimations of suspended solids from remote sensing cannot be generally solved without additional estimates of in-situ suspended solids concentration. Similarly, Weeks and Simpson (1990) indicated the importance of carefully planned optical and oceanographic measurements.

2.9   Thus although successful use has been made of empirical and semi-empirical algorithms for site and season specific studies, problems have been encountered when attempting to port these algorithms to different areas where little information exists on the *in-situ* suspended solids loading. Two factors have been proposed to explain this: firstly the differing atmospheric conditions between sites and seasons, and secondly the differing morphologies of the sediments.

2.10   The signal recorded by the remote sensing system is made up of light originating in four different ways: by scattering from below the surface (ie. the signal required) but also by reflection of skylight at the surface, by reflection of the direct solar beam at the surface, and by scattering within the atmosphere (Kirk 1983). The three additional factors contribute the majority of the signal, and are highly variable between site and season.

2.11   Differing sediment types have differing reflectance spectra, based mainly on the colour of the sediment. Thus an algorithm developed for red clay will provide inaccurate results over an area of white chalk as the spectra will be different.

2.12   Two recent advances have been made in the development of algorithms for suspended solids. Modern sensors are not restricted to fixed wavebands, with the ability to tune the wavelength ranges used dependent on the application. Additionally, many new sensor have the ability to collected data across the full spectrum, for example the CASI system records in a maximum of 288 wavebands to produce a full spectral profile. Investigations have been carried out into the exploitation of this higher spectral resolution to enable the production of a full suite of algorithms for morphology, size and colour of sediment (Shimwell, 1995). However, studies concluded that the total information within the reflectance spectrum was held within five key wavebands, minimising the number of variables which may be extracted from the data (Wernand *et al.* 1996). These studies described a technique where full spectra could be reconstructed from these 5 measured wavebands.

2.13   Secondly, atmospheric correction procedures are now being developed which claim to make the ratio type algorithms described above more globally applicable (Aiken *et al.*, 1995). Presently these are only in the developmental stage, but should shortly be available for application to data from the CASI system. One advance which this atmospheric correction procedure has revealed is the use of near infrared channels for the estimation of suspended solids concentration (Hudson *et al.* 1994).

3. ENVIRONMENT AGENCY REQUIREMENTS

3.1   In response to the requirements of the Environment Agency discussed in Section 1 above, the repeatability and wide scale (coastal zone) applicability of any algorithms developed for CASI data are of greater importance than the ability to monitor small changes. The lowest concentration to which Environment Agency laboratories report is 3 mg/l, with divisions of 0.5 mg/l above this. This is therefore the lowest division to which any airborne algorithm need measure for comparable results, with measurement to the nearest 3 mg/l acceptable for many applications.

3.2   Development of an algorithm for suspended solids from a wide data set of diverse sediment concentrations may provide a single algorithm with which to calibrate CASI data. It is necessary to assess the accuracy of such an algorithm and report on the likely errors that will be incurred during routine calibration. Alternative forms of the algorithm may be used for specific areas of coastline to overcome some of the greater errors.

3.3   In order to develop a robust algorithm it is necessary to have a wide range in suspended solids concentration. Study sites used were the Bristol Channel and the Holderness coast. The Bristol Channel has previously recorded a steep gradient in suspended solids away from the River Severn, with a distinct front between estuarine and coastal water noted around Minehead (NC/MAR/016/9). The Holderness coast has previously shown a strong offshore gradient in suspended solids loading, with very low concentrations recorded only 2 km offshore (NC/MAR/016/4). Additionally, the algorithm development was carried out on data collected from the Norfolk coast as part of an accompanying case study to optimise the calibration of CASI data for chlorophyll-*a* concentration.

3.4   In order to monitor the full variability of the suspended solids concentration, the survey design incorporated flightlines and ship tracks both parallel and perpendicular to the coastline. As described previously, the Holderness coast in particular shows a strong gradient in suspended solids profile away from the coastline, with the Bristol Channel site showing a strong gradient along the coast, decreasing with distance from the Severn Estuary.

4. DATA COLLECTION

4.1 Data were collected from the three study sites throughout 1996. The data sets used in the production and validation of algorithms to calibrate CASI imagery for suspended solids concentration are shown in Table 1. These four data sets fulfilled the criteria for algorithm development discussed in section 3.3.

Site	Date	Range of chlorophyll-a	Range of suspended solids
Norfolk	30/05/96	4.9 - 16.08 μg/l	<2 - 24 mg/l
Holderness	19/08/96	0.71 - 3.15 μg/l	<1.5 - 59 mg/l
Bristol Channel	24/06/96	-	<0.75 - 24 mg/l
Bristol Channel	12/09/96	0.58 - 2.37 μg/l	<1.5 - 90 mg/l

Table 4.1   Data collection exercises used in algorithm development

4.2 The range of suspended solids concentration was large for both the Holderness Coast and the Bristol Channel sites, with maximum concentrations greater than 90 mg/l and minimum concentrations less than the laboratory minimum reporting value of 1.5 mg/l.

4.3 Data collection exercises consisted of an integrated aerial and shipborne campaign. The airborne campaign consisted of overflights with the CASI sensor operating in enhanced spectral mode. This records 72 spectral channels of approximately 8 nm bandwidth, extending from 400 nm - 920 nm. The swath width of 402 pixels, results in a spatial resolution of 20 m at 10,000 ft altitude.

4.4 Simultaneously with overflights, a research vessel traversed the area beneath the flightlines. One litre water samples were taken at 1 m depth for laboratory analysis of suspended solids concentration. Both total and inorganic suspended solids concentration were determined using gravimetric analysis. In addition samples were analysed for chlorophyll-a concentration, in order to establish if the presence of varying degrees of organic load alter the action of the algorithms.

4.5 Additionally, continuous measurements of either %transmission or turbidity units were recorded from a towed body were instrumentation allowed. These systems recorded measurements every ten seconds.

5. CALIBRATION METHODOLOGY

5.1 TECHNICAL REQUIREMENTS

5.1.1 In order to fully develop an algorithm to calibrate CASI imagery for suspended solids concentration, at least three surveys should have been completed where good quality[1], spatio-temporally coincident[2] boat (continuous transmission or turbidity readings and laboratory samples) and airborne (CASI enhanced spectral data) data were collected, from geographic areas where suspended solids concentrations varied by at least 12 mg/l over a 20 km stretch of water.

[1]*Good quality:*   *Laboratory data - laboratory data samples must be quality assured; date, time and location of sample must be known; extreme values (eg. > 80 mg/l suspended solids) must be checked with laboratory.*

                                    Continuous transmission/turbidity data - continuous transmission or turbidity measurements must have associated date, time and location; data must be free of noise and spurious peaks and troughs.

                                    Airborne CASI data - images must be geo-corrected; date and time must be known; edge brightening and glint must be minimal; image must be free of clouds

[2]*Spatio-temporally coincident:*   *At least ten transmission or turbidity readings must be recorded within a 250 m radius of each laboratory sample site location. These are to have been recorded within 30 minutes of the laboratory sample being taken. At least 15 km of continuous track transmission or turbidity readings must lie geographically within the area of the airborne CASI data.*

5.1.2 Continuous transmission or turbidity measurements must be able to be associated spatio-temporally with at least seven laboratory samples, of which at least six must have suspended solids concentrations greater than the laboratory limit of detection.

5.1.3 A number of data collection exercises were carried out over the three sites. However, only three data sets fulfilled the criteria for algorithm development, with a further two data sets being suitable for validation of algorithms. The Norfolk Coast site provided two high quality data sets with the correct range in suspended solids concentration. The data from 30th May 1996 were used for algorithm development with these algorithms being tested on data from 11th August 1996. The Bristol Channel site also provided two data sets: the 24th June 1996 being used for algorithm development and the 12th September 1996 used for validation. The data from the Holderness coast was of lesser quality. On 19th August 1996, the continuous transmission data were noisy and smoothing techniques had to be applied. There was no second data set on which to validate algorithms, as there were no coincident imagery and laboratory data.

5.2 THEORETICAL ASSUMPTIONS

5.2.1 A number of theoretical assumptions must be made prior to the calibration of imagery. Firstly, it is assumed that laboratory samples for suspended solids (measured in mg/l) are reliable and representative of the body of water around the sample site. Continuous transmission measurements are reported in units of percentage transmission, and continuous turbidity measurements must be recorded in nephelometric turbidity units.

5.2.2 The relationship between laboratory samples and spatio-temporally associated continuous transmission measurements must show a significant negative correlation (relationship between laboratory, samples and spatio-temporally continuous turbidity must show a significant positive correlation).

5.2.3 It is assumed for this algorithm development that the relationship between laboratory samples (*Lab*) and continuous track transmission (*Trans*) or turbidity (*Turb*) may then be modelled using either linear or non-linear regressions.

5.2.4 The relationship between transmission (*Trans*) and suspended solids is most commonly logarithmic, but is linear from approximately 7.5 mg/l until saturation of transmission occurs above approximately 50 mg/l. Calibration of *Trans* to mg/l of suspended solids may therefore be expressed by the following regression equation :

$$trans(mg/l) = (m \times ln(trans)) + c$$

5.2.5 The relationship between turbidity (*Turb*) track data may best be represented by the linear equation:-

$$turb(mg/l) = (m \times turb) + c$$

5.2.6 It is also assumed that a significant relationship exists between the image data surface and the continuous track data calibrated for suspended solids. This image surface will take the form of a ratio of two of the 72 channels of enhanced spectral data.

5.2.7 The relationship between the ratio images and the calibrated continuous suspended solids data may be modelled using either linear or non-linear regression. Calibration of the ratio images to mg/l of suspended solids (at 105°C) may therefore be expressed by the following linear regression equation :-

$$casi(mg/l) = (rS \times \frac{(sd.solids)}{(sd.casi)} \times casi) + (mn.solids - (rS \times \frac{(sd.solids)}{(sd.casi)} \times mn.casi))$$

7

where rS = correlation coefficient between calibrated continuous suspended solids data and the CASI image ratio

$sd.solids$ = standard deviation of calibrated continuous suspended solids data

$sd.casi$ = standard deviation of CASI image ratio

$mn.solids$ = mean of calibrated continuous suspended solids data

$mn.casi$ = mean of CASI image ratio

This may be simplified to the following equation:

$$casi(mg/l) = (mS \times casi) + cS)$$

where:

$$mF = rF \frac{(sd.solids)}{(sd.casi)}$$

and:

$$cS = mn.solids - (rS \times \frac{(sd.solids)}{(sd.casi)} \times mn.casi)$$

5.2.8   Alternatively non-linear regression equations may be used, for example an exponential equation. These would have the following form:

$$casi\,(mg/l) = \exp(a + (b \times casi))$$

5.3   PRE-PROCESSING OF CASI IMAGERY

5.3.1   CASI imagery was radiometrically calibrated to spectral radiance units. An empirical correction was then applied to account for the enhanced brightening of the imagery at the edge. This brightening results from the increased pathlength of the signal at the edge of the image caused by the wide field of view of the instrument.

5.3.2   This empirical correction is similar to the Rayleigh step applied as part of a typical atmospheric correction. A full atmospheric correction was also applied to the data sets using software developed by Plymouth Marine Laboratory under an Environment Agency Research and Development. Previous work has suggested that the removal of

8

atmospheric effects is an essential pre-requisite for the retrieval of geophysical parameters from aerial surveillance data (Aiken *et al.*, 1995).

5.3.3   The images were first order geometrically rectified using data from the on-board ground positioning system. Second order geo-rectification was carried out using a series of ground control points to provide an accurate fit with the Ordnance Survey Grid.

5.3.4   The applicability of channel ratio algorithms for calibrating imagery for suspended solids was investigated by producing a ratio of each of the 72 channels of the enhanced spectral data against the others. These channel ratios are then taken forward into the calibration process.

5.3.5   As stated, previous work suggests that the relationship between suspended solids and aerial imagery will be dependent on the atmospheric conditions at the time of measurement. Thus removal of the atmospheric effects from the reflectance signal measured by the CASI instrument should ensure that algorithms are more widely applicable.

5.3.6   Software developed by Plymouth Marine Laboratory was used to remove atmospheric effects from the data sets collected for algorithm development (see Table 1). As this software is unable to correct enhanced spectral imagery, the images were compressed into 15 bands simulating the Environment Agency coastal bandset.

5.3.7   The ratios between each of the fifteen channels of the atmospherically corrected data were calculated as these ratio images were used in algorithm development.

5.4   ASSESSMENT OF ERRORS

5.4.1   In order to rigorously investigate the errors, the systematic and random uncertainties were calculated to allow an assessment of the most accurate algorithm. This will provide a clear indication of the most suitable algorithm for global use.

5.4.2   The data set was split into odd and even numbered pairs of observations, giving two subsets, each spanning the whole range of suspended solids concentration encountered. The even data set was used to establish the best relationship between imagery and both laboratory and continuous data, and the resultant equation was used to transform the odd data set to predicted suspended solids concentrations. The differences were used to calculate the mean bias (ie. the systematic error) and the variability about the mean (ie. the random error), as in BS5844.

6. CALIBRATION RESULTS

6.1 LABORATORY TO CONTINUOUS TRANSMISSION/TURBIDITY DATA REGRESSION

6.6.1 The best correlations between laboratory samples and continuous data tended to occur with continuous track data lying within a 100 metre and thirty minute buffer of the laboratory sampling sites, the exception being the Norfolk data set. Therefore 100 metre buffers where used in the calibration of the continuous track data. The following tables show how the correlation coefficient varies with the size of the distance buffer selected.

Table 6.1   Bristol Channel, 24th June 1996

Size of buffer	Number of samples - n	Correlation coefficient - r
coincident cells	16	-0.90843
50 m	72	-0.95064
100 m	**111**	**-0.96011**
150 m	133	-0.94827
200 m	161	-0.94568
250 m	174	-0.9438
300 m	194	-0.94298
400 m	229	-0.93754
500 m	260	-0.93729
750 m	346	-0.92867
1000 m	469	-0.9289

Table 6.2   Holderness Coast, 19th August 1996.

NB: raw transmission was noisy, therefore a smoothing algorithm was used - 13 record lateral mean filter, excluding lower and upper 20 percentiles.

Size of buffer	Number of samples - n	Correlation coefficient - r
100 m	**37**	**-0.62139**
200 m	72	-0.59144
300 m	107	-0.60176
400 m	139	-0.60941

Table 6.3   North Norfolk Coast, 30 May 1996.
NB: Calibration is against turbidity as apposed to transmission. A positive correlation is therefore expected.

Size of buffer	Number of samples - n	Correlation coefficient - r
100 m	118	0.741285
250 m	520	0.782345

6.6.2   Best fit regression equations for the calibration of continuous transmission or turbidity data to laboratory suspended solids (at 105°C) equivalence have been calculated for the three test sites: the Holderness coast, the Bristol Channel and the North Norfolk coast, and are displayed in table 5.

Table 6.4   Algorithms to calibrate continuous transmission or turbidity data to suspended solids for each of the three sites

Test site	Type	Date	n	r	regression type	m	c
Holderness	transmission	19/08/96	37	-0.62	non-linear	-19.94	
equation: transmission as ss@105 °C = (n × ln(transmission)) + c							
Bristol Channel	transmission	24/06/96	111	-0.96	non-linear	-5.21	
equation: transmission as ss@105 °C = (n × ln(transmission)) + c							
Norfolk	turbidity	30/5/96	118	0.74	linear	3.53	
equation: turbidity as ss@105 °C = (m × turbidity) + c							

6.2   CONTINUOUS DATA TO IMAGE DATA REGRESSION

6.2.1   Individual image algorithms

6.2.1.1   The correlation coefficient between the ratio of each pair of channels and calibrated continuous track data is displayed in the matrix plots shown in figures 1 to 9. The two channels, which when ratioed, produce the highest positive correlation with the calibrated transmissometer or turbidity data, are those which show as red in each matrix. The matrix also shows the inverse ratios which produce a negative correlation of the same magnitude. Slight differences in the duplication of the matrix are due to computational rounding errors.

6.2.1.2   Comparison of the matrices of different images allows the identification of channel ratios which show a consistent correlation with suspended solids concentration. A consistent correlation between images would suggest a ratio which would be suitable for the calibration of a set of algorithm.

6.2.1.3   The sea truth data corresponding to two of the images (one from the Bristol Channel and one from the Norfolk coast) showed low concentrations of suspended solids, whilst the concentrations elsewhere were high and varied. One image from the Bristol Channel had some glint and edge brightening. The images collected for the Holderness site represent two sorties over each of two flightlines, with one sortie corresponding more closely to the time of sea truth data collection.

6.2.1.4   Each matrix shows a similar pattern, although with differing strength, with two predominantly positively correlated areas at approximately red against near-infrared, and at red against blue. These areas have corresponding negative correlations where the reverse ratios occur.

6.2.1.5   The red against blue ratios show the strongest correlations for the Holderness images, but for all the images the red against near-infrared ratios show high correlations. The ratio of red against near infrared was therefore selected for subsequent algorithm development, as this was most representative of the three cases.

6.2.2 Site specific (local) algorithms

6.2.2.1   In order to calculate a calibration algorithm for each of the three sites, coefficients from the correlation/regression matrices of the individual images covering this area were averaged for each ratio. The Holderness data were treated as two separate data sets due to the difference in timing. Figures 10 to 14 show the averaged correlation coefficients for the areas.

6.2.2.2   The relationships between the red and near-infra-red ratios are highlighted as being strongly correlated. The following table shows some of the results that can be used to calibrate the imagery as local algorithms using the equation:

$$casi(mg/l) = (mS \times casi) + cS$$

6.2.2.3   The correlation coefficient, r, in this Pearson regression analysis is a comparison between two independent variables. The value of r which is statistically significant varies depending on the sample size.

Table 6.5   Selection of site specific algorithms

Area	Band ratio	r	m	c	Algorithm selected
Norfolk	25 / 49	0.44	43.81	-91.32	
	26 / 49	0.44	43.81	-91.76	
	26 / 50	0.44	38.81	-82.63	
	27 / 49	0.44	49.36	-91.77	
	27 / 50	0.44	44.22	-84.70	*
Bristol Channel	30 / 50	0.55	2.86	-3.38	
	31 / 50	0.56	2.94	-3.30	
	36 / 50	0.55	3.31	-2.60	
	37 / 50	0.56	3.39	-2.60	*
	39 / 50	0.56	3.57	-2.63	
Holderness (all images)	44 / 50	0.70	36.36	-35.53	
	35 / 50	0.65	21.76	- 28.00	
	39 / 50	0.68	24.11	-29.11	
Holderness (coincident images)	35 / 50	0.65	15.79	-20.82	*
	30 / 50	0.60	15.15	-25.39	

6.2.2.3   The algorithms chosen were based not only on the strength of the correlation, but also on the bands in the ratio and adjacent bands correlation, (ie. to make sure that the high correlation of the ratio is not a statistical outlier). Also equations with lower values for the constant in the linear equation (c) were favoured in order that the multiplicant had more influence on the results.

6.2.3   Atmospherically corrected data algorithms

6.2.3.1   The image data sets for each case study site were corrected for the effects of the atmosphere, resulting in 15 band imagery, as described in section 5.6. The ratio between each band was again calculated and the relationship between each ratio in this matrix with suspended solids concentration calculated.

6.2.3.2   Figures 15 to 20 show the correlation matrices for the band ratios for each atmospherically corrected CASI image against continuous track data calibrated to suspended solids.

13

6.2.3.3 For each wavelength, the correlation between calibrated suspended solids and the band ratio was lower than that found prior to the removal of atmospheric effects. Moreover, the strong correlation between suspended solids and the red to near-infrared band ratio is no longer apparent. The highest correlations are noted between suspended solids and the red to blue/green band ratio.

6.2.3.4 The low correlation coefficients found meant that the further development of site specific and global algorithms has not been undertaken, with atmospherically corrected imagery. Similarly, non-linear exponential algorithms were developed with the non-atmospherically corrected data set.

6.2.4 An exponential equation

6.2.4.1 The scatter plots of channel ratio against suspended solids concentration showed that the linear regression may not provide the optimum fit to the data. Various other curves were therefore fitted to the data sets in order to best represent the scatter, with the exponential curve providing the best fit. Tables 6.6 to 6.8 show the calibration constants and correlation coefficients for each channel ratio tested.

Band ratio	a	b	r^2
25 / 49	**-5.356**	**3.426**	**0.592**
26 / 49	-4.863	3.251	0.531
26 / 50	-4.475	2.960	0.555
27 / 49	-5.142	3.746	0.517
27 / 50	-4.445	3.292	0.540
28 / 49	-4.530	3.675	0.473
28 / 50	-4.107	3.324	0.500
30 / 50	-3.959	3.529	0.382
31 / 50	-3.503	3.436	0.376
33 / 50	-3.078	3.568	0.370
36 / 50	-3.248	4.010	0.309
37 / 50	-2.931	3.875	0.301
39 / 50	-3.014	4.075	0.268

Table 6.6 Calibration constants and correlation coefficients for Image 1875

Band ratio	a	b	r^2
25 / 49	**-5.920**	**3.607**	**0.619**
26 / 49	-5.811	3.582	0.605
26 / 50	-5.213	3.194	0.590
27 / 49	-6.074	4.121	0.592
27 / 50	-5.235	3.581	0.578
28 / 49	-6.053	4.321	0.558
28 / 50	-5.518	3.887	0.554
30 / 50	-6.089	4.462	0.501
31 / 50	-5.920	4.539	0.492
33 / 50	-5.570	4.821	0.470
36 / 50	-5.904	5.489·	0.441
37 / 50	-5.848	5.512	0.425
39 / 50	-5.962	5.782	0.386

Table 6.7 . **Calibration constants and correlation coefficients for Norfolk Coast image mosaic**

6.2.4.2 Exponential algorithms were developed for the two individual images which showed the best linear correlation, one from the Bristol Channel and one from the Norfolk coast, and additionally for a mosaic of three images from the Norfolk Coast. This image mosaic was produced for a parallel case study to investigate the development of algorithms for chlorophyll-*a* (Environment Agency, 1997). The correlation coefficient for this mosaic was found to be much greater than for the individual images.

6.2.4.3 Exponential equations provided highly accurate fits to the calibration data sets. Image 2061 from the Bristol Channel recorded the best correlation between the ratio of channels 31 and 50 and suspended solids, with an r^2 value of 0.814. The best correlation in Norfolk, for both the individual image and the image mosaic is between channels 25 and 49 and suspended solids. There is a slight increase in the correlation coefficient when all images are included in the mosaic. However, the change is not so marked as that found in the chlorophyll-a case study. This suggests that the variability in suspended solids concentration is over a scale which may be represented by one CASI image.

6.2.4.4 The calibration curves for each exponential equation are shown in figures 21

to 23. These illustrate the tighter fit of the Bristol Channel data set, and the differing slopes between the two data sets.

Band ratio	a	b	r^2
25 / 49	-1.662	0.946	0.569
26 / 49	-1.611	0.941	0.656
26 / 50	-1.732	0.928	0.658
27 / 49	-1.379	0.986	0.726
27 / 50	-1.534	0.985	0.739
28 / 49	-1.197	0.986	0.780
28 / 50	-1.301	0.972	0.789
30 / 50	-0.948	0.949	0.814
31 / 50	**-0.793**	**0.929**	**0.814**
33 / 50	-0.570	0.930	0.812
36 / 50	-0.450	0.992	0.800
37 / 50	-0.340	0.966	0.785
39 / 50	-0.309	0.999	0.789

Table 6.8   **Calibration constants and correlation coefficients for Bristol Channel image mosaic**

6.2.4.5   In figure 24 the two individual image data sets have been plotted on one graph. The channel ratio selected is that which shows the commonly best correlation in both data sets. It is immediately apparent that there are two populations within the graph. This means that the development of a global algorithm is highly unlikely to succeed using this empirical algorithms development approach.

6.2.5 A global linear algorithm

6.2.3.1   Although it is unlikely that a global algorithm would provide adequate results for the calibration of CASI imagery for suspended solids concentration, an attempt was made to establish such an algorithm so that the errors which would be incurred could be accurately assessed. This development was carried out using a linear algorithm as this was computationally more simple. Additionally

the linear algorithm is likely to be more portable as the equation has less variables.

6.2.3.2   In order to calculate the global calibration algorithm, coefficients from the local sites correlation/regression matrices were averaged for each ratio. Figure 16 shows the global averaged correlation coefficients.

6.2.3.3   Again, the relationship between red and near-infrared ratios is highlighted as being the most strongly correlated to the sea truth suspended solids data. The following table shows some of the results that can be used to calibrate the imagery as a global algorithm. Band 50, corresponding to 754 nm, or very near- infrared, is the divisor for all the ratios here, and for most of the previously highlighted ratios.

Table 6.9   Selection of global algorithm

Area	Band ratio	r	m	c	Algorithm selected
Global	31 / 50	0.52	22.60	-36.05	
	33 / 50	0.52	23.96	-34.27	*
	37 / 50	0.53	25.39	-32.05	.

6.2.3.4   The global algorithm for calibrating CASI enhanced spectral data to mg/l of suspended solids was selected as that which ratioed band 33 with band 50, as band 33 was at the centre of the bands used for the local algorithms. The form of the global algorithm is:

$$casi(mg/l) = (23.96 \times \frac{(channel\ 33)}{(channel\ 50)}) - 34.27$$

6.2.3.5   The magnitude of the errors incurred by applying this algorithm to both calibration and validation data sets is discussed in section 6.4.

6.4 CALIBRATION OF CASI IMAGERY FOR SUSPENDED SOLIDS CONCENTRATION

6.4.1 Introduction

6.4.1.1   A suite of algorithms have been developed to relate image ratios to suspended solids for individual images and on a site specific basis. Additionally, a global linear algorithm has been developed. The results of applying each of these algorithms to both the calibration and validation data sets from the Bristol Channel site and the Norfolk coast site are described below. The high levels of noise in the Holderness coast site mean that the algorithms have not been applied to this data set.

6.4.1.2   The mean and random errors incurred when applying each algorithm are compared against those using traditional laboratory gravimetric analysis. The mean error for the determination of suspended solids concentration in laboratory analysis is 10% of the suspended solids concentration, with a random error of 12%. Thus for an average suspended solids concentration of 10 mg/l the mean error, or bias, would be 1 mg/l and the random error would be 1.2 mg/l.

6.4.1.3   Table 6.10 shows the mean and random errors incurred by applying each algorithm.

6.4.2 Bristol Channel data sets - 24th June 1996 and 12th September 1996

6.4.2.1   Figures 25 and 26 show the results of applying the different linear algorithms to the calibration data from the Bristol Channel. The image specific and local algorithms give similar spatial results. The results in table 6.10 show that both linear algorithms give a good fit for this calibration data set, with mean errors of 0.77 mg/l and 1.196 mg/l when compared with calibrated transmission values. The random errors of 1.099 mg/l and 2.403 mg/l compare well with the laboratory errors of 1.2 mg/l. Correlation against laboratory samples is lower with a random error of 2.991 mg/l or 3.833 mg/l depending on algorithm.

6.4.2.2   The image specific exponential algorithm gives a slightly improved fit over the image specific linear algorithm, with a mean error of 0.751 mg/l and a random error of 1.117 mg/l. Again the correlation with laboratory samples is lower than that with calibrated transmission data. The application of this exponential algorithm is illustrated in figure 27.

6.4.2.3   The global linear algorithm developed with data from the Bristol Channel, the Norfolk Coast and the Holderness Coast gives a poor correlation when applied to the Bristol Channel calibration data set, with a mean error of 17.242 mg/l

Table 6.10 Error Estimation Statistics For Suspended Solids to Imagery Calibration Algorithms

Data Type	Image	Calibrated SS@105 Surface	Ground Truth Data	Date	count	Mean Ground Truth Data /---------(mg/l SS@105°C)---------\	Std. Dev Ground Truth Data	Absolute Error (mg/l SS@105°C Equivalent) Mean (Standard Error)	Standard Deviation	Minimum	5%-tile	95%-tile	Maximum	Random Error
Calibration	1875 (Norfolk)	Image Specific Linear	Calibrated Turbidity	30th May 1996	579	28.342	24.082	11.638	11.325	0.056	0.752	33.640	75.741	22.310
Calibration	1875 (Norfolk)	Image Specific Linear	Lab. Data (100m buffer)	30th May 1996	138	13.000	3.000	7.042	4.944	0.002	0.701	15.876	24.463	9.739
Calibration	2061 (Bristol)	Image Specific Linear	Calibrated Transmission	24th June 1996	239	5.586	2.191	0.770	0.558	0.006	0.088	1.853	2.678	1.099
Calibration	2061 (Bristol)	Image Specific Linear	Lab. Data (100m buffer)	24th June 1996	324	6.250	2.278	2.259	1.518	0.023	0.289	4.292	5.198	2.991
Calibration	1875 (Norfolk)	Local Linear	Calibrated Turbidity	30th May 1996	579	28.342	24.082	12.077	18.347	0.011	0.344	59.943	88.118	36.144
Calibration	1875 (Norfolk)	Local Linear	Lab. Data (100m buffer)	30th May 1996	138	13.000	3.000	4.171	2.530	0.065	0.534	8.242	10.440	4.984
Calibration	2061 (Bristol)	Local Linear	Calibrated Transmission	24th June 1996	239	5.586	2.191	1.196	1.220	0.001	0.054	3.565	4.681	2.403
Calibration	2061 (Bristol)	Local Linear	Lab. Data (100m buffer)	24th June 1996	324	6.250	2.278	2.558	1.946	0.003	0.033	5.450	5.815	3.833
Calibration	Norfolk Mozaic	Local Linear	Calibrated Turbidity	30th May 1996	2193	14.159	15.647	5.818	10.976	0.003	0.258	20.179	165.355	21.623
Calibration	Norfolk Mozaic	Local Linear	Lab. Data (100m buffer)	30th May 1996	464	10.495	3.213	3.749	2.274	0.002	0.461	7.874	10.440	4.479
Calibration	1875 (Norfolk)	Global Linear	Calibrated Turbidity	30th May 1996	579	28.342	24.082	19.988	22.352	0.424	2.809	75.551	105.231	44.033
Calibration	1875 (Norfolk)	Global Linear	Lab. Data (100m buffer)	30th May 1996	138	13.000	3.000	6.424	3.855	0.281	1.205	11.877	14.106	7.595
Calibration	2061 (Bristol)	Global Linear	Calibrated Transmission	24th June 1996	239	5.586	2.191	17.242	7.057	1.891	4.853	28.667	31.840	13.902
Calibration	2061 (Bristol)	Global Linear	Lab. Data (100m buffer)	24th June 1996	324	6.250	2.278	10.903	5.877	0.009	0.519	17.719	21.415	11.578
Calibration	Norfolk Mozaic	Global Linear	Calibrated Turbidity	30th May 1996	2193	14.132	15.613	8.385	14.012	0.005	0.612	31.446	166.882	27.603
Calibration	Norfolk Mozaic	Global Linear	Lab. Data (100m buffer)	30th May 1996	464	10.495	3.213	5.285	2.777	0.272	1.704	10.634	12.777	5.470
Calibration	1875 (Norfolk)	Image Specific Exponential	Calibrated Turbidity	30th May 1996	579	28.342	24.082	9.920	11.927	0.011	0.441	36.526	78.888	23.496
Calibration	1875 (Norfolk)	Image Specific Exponential	Lab. Data (100m buffer)	30th May 1996	138	13.000	3.000	5.338	3.966	0.076	0.466	12.066	20.960	7.813
Calibration	2061 (Bristol)	Image Specific Exponential	Calibrated Transmission	24th June 1996	239	5.586	2.191	0.751	0.567	0.002	0.054	1.953	2.923	1.117
Calibration	2061 (Bristol)	Image Specific Exponential	Lab. Data (100m buffer)	24th June 1996	324	6.250	2.278	2.229	1.497	0.037	0.253	4.499	5.079	2.949
Calibration	1875 (Norfolk)	Local Exponential	Calibrated Turbidity	30th May 1996	579	28.342	24.082	9.246	12.207	0.002	0.409	39.328	82.151	24.048
Calibration	1875 (Norfolk)	Local Exponential	Lab. Data (100m buffer)	30th May 1996	138	13.000	3.000	4.309	3.053	0.022	0.407	9.619	15.645	6.014
Calibration	Norfolk Mozaic	Local Exponential	Calibrated Turbidity	30th May 1996	2193	14.132	15.613	5.128	8.323	0.002	0.266	15.849	161.339	16.396
Calibration	Norfolk Mozaic	Local Exponential	Lab. Data (100m buffer)	30th May 1996	464	10.495	3.213	2.832	2.374	0.007	0.269	7.215	15.645	4.678
Validation	Norfolk Mozaic	Local Linear	Lab. Data (100m buffer)	11th August 1996	872	5.441	10.978	7.368	7.527	0.003	0.601	29.235	32.405	14.829
Validation	Bristol Mozaic	Local Linear	Lab. Data (100m buffer)	12th September 1996	526	7.144	2.895	2.282	1.149	0.367	1.017	4.919	5.584	2.264
Validation	Norfolk Mozaic	Global Linear	Lab. Data (100m buffer)	11th August 1996	872	5.441	10.978	5.016	9.635	0.000	0.276	34.765	36.010	18.980
Validation	Bristol Mozaic	Global Linear	Lab. Data (100m buffer)	12th September 1996	526	7.144	2.895	29.738	11.158	0.706	13.550	49.658	53.503	21.982
Validation	Norfolk Mozaic	Local Exponential	Lab. Data (100m buffer)	11th August 1996	872	5.441	10.978	25.877	20.737	0.009	8.598	69.623	157.653	40.852
Validation	Bristol Mozaic	Local Exponential	Lab. Data (100m buffer)	12th September 1996	526	7.144	2.895	4.037	3.879	0.006	0.301	13.285	17.302	7.641

and a random error of 13.902 mg/l. Application of the algorithm is illustrated in figure 28, which clearly shows the over-estimation of suspended solids concentration using this algorithm.

6.4.2.4   The algorithms were then applied to data collected from the Bristol Channel on 12th September 1996 to assess the seasonality of the algorithms. The best correlation is found with the local linear equation, giving a mean error of 2.282 mg/l and a random error of 2.264 mg/l. This compares extremely well with the laboratory accuracies and demonstrates the portability of this algorithm between different data collection exercises at the Bristol Channel site. This is illustrated in figure 29. The image specific exponential algorithm also gives a reasonable correlation, although the mean error of 4.037 mg/l and the random error of 7.641 mg/l exceed the laboratory accuracies. Application of the global algorithm results in poor results, with a mean error of 29.738 mg/l and a random error of 21.982 mg/l.

6.4.3 Norfolk Coast data sets, 30th May 1996 and 11th August 1996

6.4.3.1   The mean and random errors resulting from calibration of images from the Norfolk Coast are higher than those encountered in the Bristol Channel. These algorithms were developed using the calibrated turbidity data. This data set correlated with laboratory samples with a correlation coefficient of 0.78. This correlation, although significant, is not particularly suitable for predictive modelling of suspended solids concentration. This is clearly shown in the fact that the correlation in this case is higher against laboratory samples.

6.4.3.2   The results of applying the linear local algorithm to the North Norfolk Coast data from 39th May is illustrated in figures 30. The two linear algorithms give a similar range of suspended solids concentrations with the same spatial pattern of variation. The image specific algorithm gives a mean error of 7.042 mg/l, with mean errors of 4.171 mg/l and 5.818 mg/l when the local algorithm is used. These errors are greater than those found using traditional laboratory analysis. Similar errors are encountered when the exponential algorithm is applied, both to the individual image and the image mosaic. Figure 31 illustrates the application of the exponential algorihtm to the calibration data sets.

6.4.3.3   The global algorithm results in similar mean errors as those encountered in the Bristol Channel data, with mean errors of 19.988 mg/l for the individual image 1875 and 8.385 mg/l for the image mosaic. The application of this algorihtm is shown in figure 32.

6.4.3.4   The algorithms deevloped for 30th May are not porable to imagery collected in the same area on 11th August. A mean error of between 5.016 mg/l and 25.877 mg/l results.

7. DISCUSSION

7.1 The algorithm development described above has taken an hierarchical approach, by firstly calibrating the continuous transmission or turbidity data for suspended solids concentration by reference to laboratory spot sample results, and secondly using these continuous data to calibrate the aerial CASI imagery.

7.2 Statistically highly significant correlations were found between the continuous data and the laboratory samples of suspended solids for each of the case study sites, with a negative non-linear correlation between transmission and suspended solids and a positive linear correlation between turbidity and suspended solids. The correlation between laboratory samples and turbidity was not high enough for accurate predictive modelling of suspended solids concentration and the Holderness Coast data set showed high levels of noise making it unsuitable for algorithm development. Transmission was therefore selected as the best variable to build up a suspended solids relationship.

7.3 The statistically high correaltion between laboratory water samples and transmission found in the Bristol Channel data set is thought to be due to the dominance of mineral suspended solids compared with organic solids in this region. In areas where there are high levels of organic matter calibration of % transmission is less reliable (Shimwell, *pers. comm.*). This enabled calibration of all continuous sampling data to suspended solids to be applied, maximising the number of samples with which to calibrate the aerial CASI imagery.

7.4 A thorough investigation was carried out into the linear relationship between any ratio of the 72 CASI bands and the concentration of suspended solids. For each image a number of statistically significant correlations were found, which allowed progression to the development of an algorithm for each study site: Holderness, north Norfolk coast and the Bristol Channel.

7.5 The highest correlation was found between suspended solids and the red to near-infrared band ratio. This may be explained by the shape of reflectance spectra collected over turbid waters. Clear water absorbs all sunlight in near-infrared, whereas the presence of sediment within the water column results in enhanced scattering at these wavelengths. Thus the value of reflectance recorded in the near-infrared should relate directly to the suspended solids concentration (Hudson *et al.* 1994). Suspended solids also cause a peak in reflectance at red wavelengths, with the exact position of the peak relating to the colour of the sediment. Thus both wavelengths in this ratio are dependent on the suspended solids concentration.

7.6 The scatter plots of suspended solids concentration against channel ratio clearly showed that a curve would provide a better fit to the data than the linear equation. A number of curves were fitted to the data, with an exponential curve providing the statistically best fit to the data. Application of these algorithms resulted in increased accuracy of prediction both for the validation and calibration data sets.

7.7 The effects of atmospheric interference have previously been considered to be so great that their removal is considered an essential pre-requisite for the utilisation of remotely sensed data (Aiken *et al.*, 1995). This led to the establishment of a collaborative contract with Plymouth Marine Laboratory to establish procedures for the atmospheric correction of Environment Agency CASI data.

7.8 The algorithms developed from this contract were applied to the CASI images collected from the case study sites. Although there was generally a statistically significant correlation between the reflectance in these images and suspended solids, the value of this correlation was found to be substantially lower than that with the non-atmospherically corrected data. The best relationship was found to exist between suspended solids and the red to blue wavelengths. The significance of this may again be explained by the higher reflectance of red light.

7.9 The accuracy with which each algorithm could predict the suspended solids concentration was assessed by splitting the data set into two and using half to develop a calibration and the other half as a test data set. The results of this showed that both the linear and the exponential algorithms for the Bristol Channel data set showed mean and random errors comparable with that found by traditional laboratory techniques when the image data was correlated with the calibrated transmission data. The major errors occur on moving from gravimetric suspended solids measurement to either boat or air derived optical transmission.

7.10 Low mean and random errors were also found when the linear algorithms developed for the Bristol Channel site on 24th June 1996 were applied to data collected from the same site on 12th September 1996. The exponential algorithm proved to be less portable between data collection exercises, due to the complexity of the equation. The high accuracy of the linear algorithm shows the clear potential for establishing a local algorithm for this site for routine calibration of CASI imagery.

7.11 The algorithms did not produce the same level of accuracy when applied in the same way to the Norfolk data sets. Again the major errors occurred when moving from gravimetric to optical methods, but the degree of correlation was worse with this turbidity data than was found with transmission data. This is due to the different measuring techniques used by the two systems, with turbidity being a measure of side scattered light which is influenced by the number of particles and transmission being a measure of the actual amount of sediment within the measurement path.

7.12 Site specific algorithms for the calibration of CASI imagery to suspended solids concentration have been developed with statistically high correlations against calibrated transmission data. These algorithms show some portability between different surveillance events at the same site. However, the development of a global algorithm for the routine calibration of CASI imagery proved unsuccessful, with atmospheric correction actually decreasing the portability. Scatter plots showed that the Bristol Channel and Norfolk Coast optical data sets were clearly different and could not be reconciled in one common relationship.

8. CONCLUSIONS

- The development of algorithms to calibrate CASI imagery for suspended solids are highly significantly correlated with reference results and can allow estimation of suspended solids with comparable accuracy with traditional laboratory techniques. These techniques allow the visualisation of suspended solids concentration gradients over a wide spatial scale.

- The algorithm developed for the Bristol Channel site proved to be portable to data collected later in the year. Algorithms for the Norfolk Coast, however, proved not to be portable. Presently accepted image processing technique such as atmospheric correction were not able to improve matters.

- The algorithms were found to be site specific and could not be used to calibrate CASI data from a different site. This may be due to difference in morphologies between the two data collection sites. However, the portability of algorithms to data from a different date but similar location means that a suite of algorithms could be developed for different sections of the coastline removing the requirement for costly boat calibration data.

- The correlation between laboratory samples and turbidity is not of a high enough accuracy for algorithm development. Transmission data is preferred for this type of work.

- Despite the failure of presently accepted image processing techniques, the difference in the accuracy with which the linear and exponential equations fit the data sets show that there is room for improvement in the algorithm accuracy. More innovative procedures such as chemometric techniques should be investigated in order to improve the correlation.

9. RECOMMENDATIONS

- A suite of algorithms should be developed to calibrate CASI imagery for differing areas of the coastline, based on the empirical algorithm development explored in this case study.

- More complex chemometric techniques should be investigated in order to improve the portability of the algorithms.

- Underway transmission data should always be collected for relating CASI imagery to suspended solids concentration.

22

10. REFERENCES

Aiken, J., Hudson, S., Moore, G. and Bottrell, H., 1995 Further development of airborne remote sensing techniques. A preliminary report to the National Rivers Authority. Plymouth Marine Laboratory, April 1995.

Brown, J. and Simpson, J.H. 1990. The radiometric determination of total pigment and seston and its potential use in shelf seas. *Estuarine, Coastal and Shelf Science.* Volume 31, pp 1-9.

Collins, M.B. and Pattiaratchi, C. 1984. *International Journal of Remote Sensing.* Volume 5, p635.

Curran, P.J., Hansom, J.D., Plummer, S.E. and Pedley, M.I. 1987. Multispectral remote sensing of nearshore suspended sediments: a pilot study. *International Journal of Remote Sensing.* Volume 8, pp 103-122.

Environment Agency, 1997. Calibration of CASI imagery for high concentrations of chlorophyll-*a* in turbid waters. National Centre for Environmental Data and Surveillance, March 1997.

Hudson, S.J., Moore, G.F., Bale, A.J., Dyer, K.R. and Aiken, J. 1994. An operational approach to determining suspended sediment distributions in the Humber Estuary by airborne multi-spectral imagery. *Proceedings of the First International Conference on Airborne Remote Sensing, Strasbourg, France. 12th - 15th September 1994.*

Kirk, J.T.O. 1983. Light and photosynthesis in aquatic ecosystems. Cambridge University Press.

Klemas, V., Borchardt, J.F. and Treasure, W.M. 1973. Suspended sediments observations from ERTS-1. *Remote Sensing of Environment.* Volume 2, pp 205-221.

Mitchelson, E.G., Jacob, N.J. and Simpson, J.H. 1986 Ocean colour algorithms from the Case 2 waters of the Irish Sea in comparison to algorithms from case 1 waters. *Continental Shelf Research,* Volume 5, no 3, pp 403-415.

Munday, J.C. and Alfoldi, T.T., 1979. Landsat test of diffuse reflectance models for aquatic suspended solids measurement. *Remote Sensing of Environment.* Volume 8, pp 169-183.

NC/MAR/016/4. National Marine Baseline Survey, 1995. Littoral Cell 2: Flamborough Head to The Wash. Environment Agency, National Centre for Environmental Monitoring and Surveillance.

NC/MAR/016/9. National Marine Baseline Survey, 1995. Littoral Cell 7: Lands End to the Severn Estuary. Environment Agency, National Centre for Environmental Monitoring and Surveillance.

Rimmer, J.C., Collins, M.B and Pattiaratchi, C. 1987. Mapping of water quality in coastal waters using Airborne Thematic Mapper data. *International Journal of Remote Sensing*, Volume 8, no 1 pp 85-102.

Ritchie, J.C., Cooper, C.M. and Scheibe, F.R., 1990. The relationship of MSS and TM digital data with suspended sediments, chlorophyll and temperature in Moon Lake, Mississippi. *Remote Sensing of Environment*. Volume 33, pp 137-148.

Shimwell, S.J. 1995 An investigation into the optical properties of north sea coastal waters in relation to ocean colour remote sensing. PhD Thesis, University of Southampton.

Stumpf, R.P. and Pennock, J.R., 1989. Calibration of a general optical equation for remote sensing of suspended sediments in a moderately turbid estuary. *Journal of Geophysical Research*. Volume 94, pp 14363-14371.

Weeks, A. and Simpson, J.H. 1990. The measurement of suspended particulate concentrations from remotely sensed data. *International Journal of Remote Sensing*.

Wernand, M.R., Shimwell, S.J. and de Munck, J.C. 1997 A simple method of full spectral reconstruction by a 5-band approach for ocean colour applications. *International Journal of Remote Sensing: Special Issue on Airborne Remote Sensing*. In press.

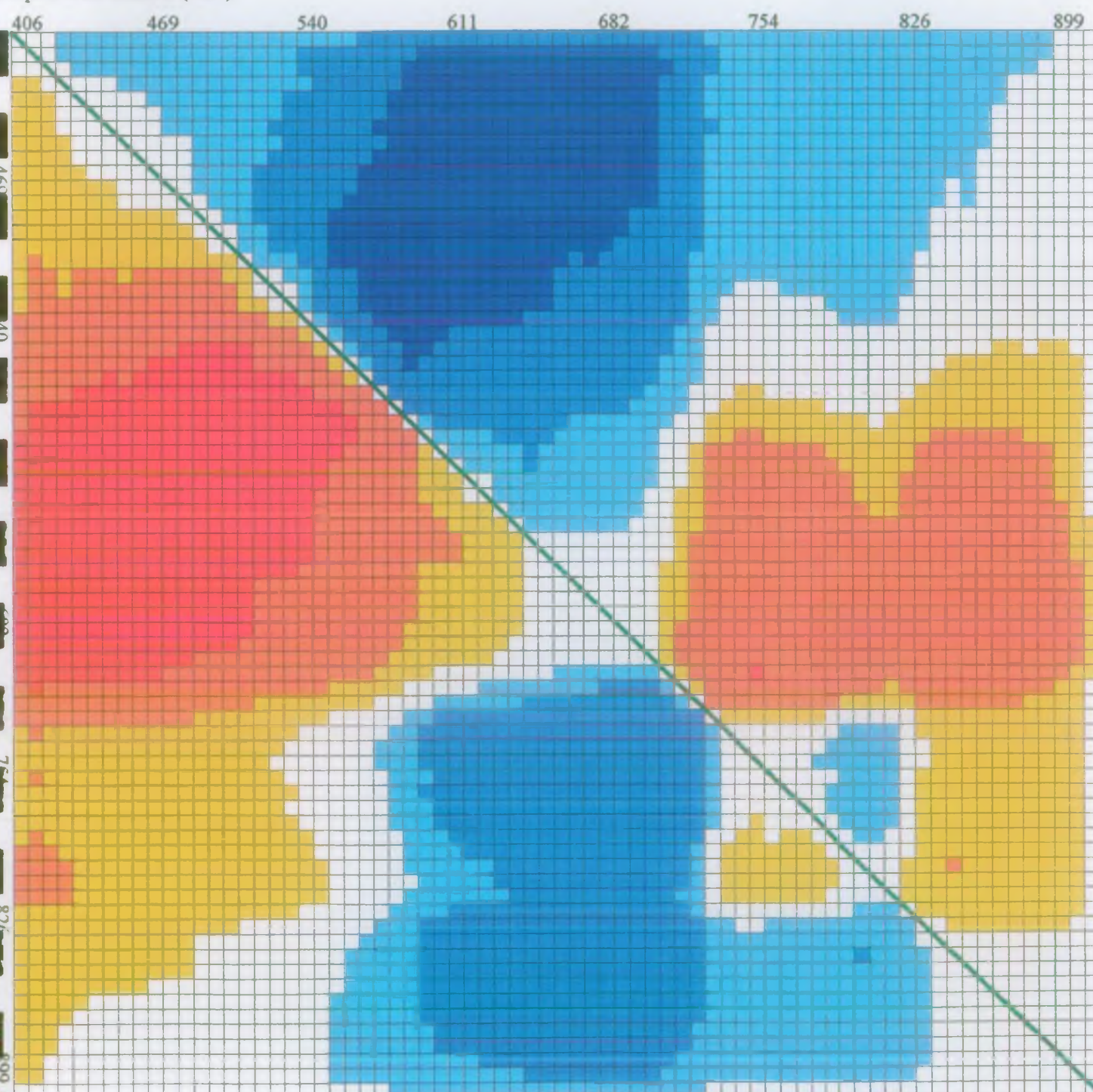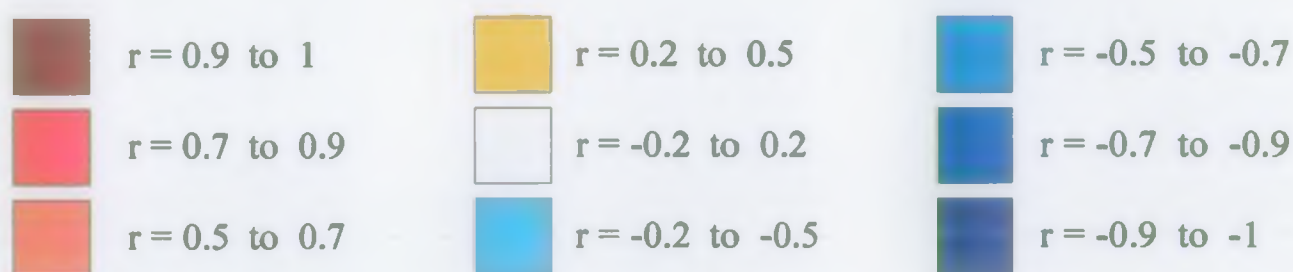**Figure 1. Correlation coefficient matrix for ratios of each band of enhanced spectral CASI image IMAG1875 compared with calibrated turbidity ground truth data from boat.**

r = 0.9 to 1
r = 0.7 to 0.9
r = 0.5 to 0.7
r = 0.2 to 0.5
r = -0.2 to 0.2
r = -0.2 to -0.5
r = -0.5 to -0.7
r = -0.7 to -0.9
r = -0.9 to -1
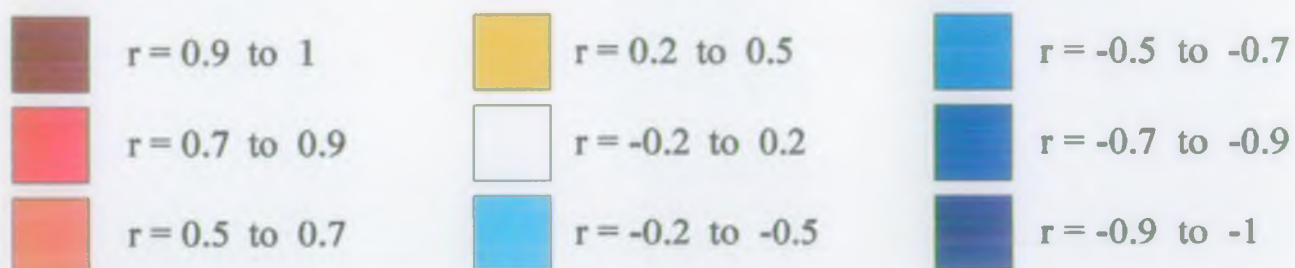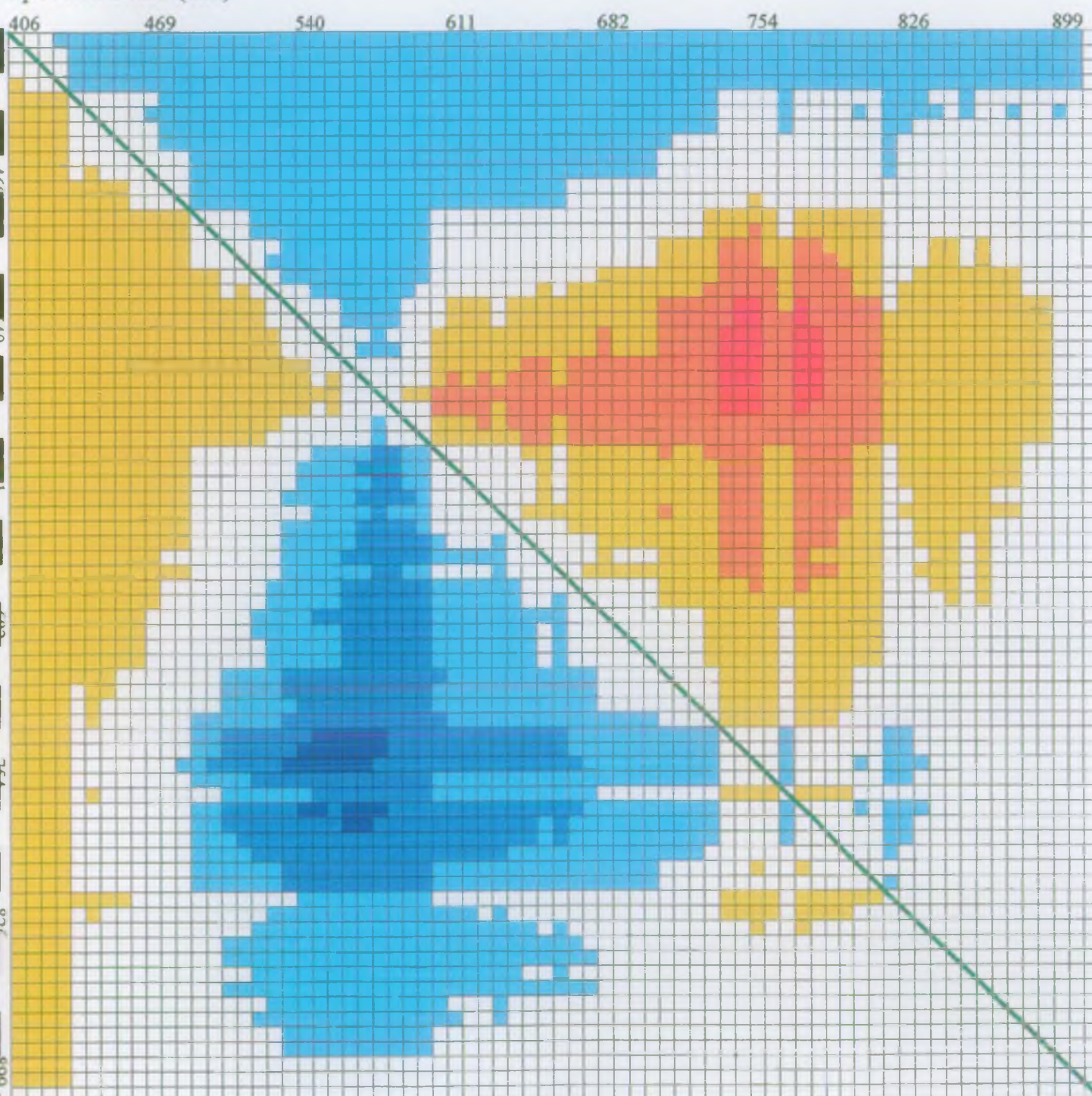
Spectral Band (nm)

Figure 2. Correlation coefficient matrix for ratios of each band of enhanced spectral CASI image IMAG1876 compared with calibrated turbidity ground truth data from boat.
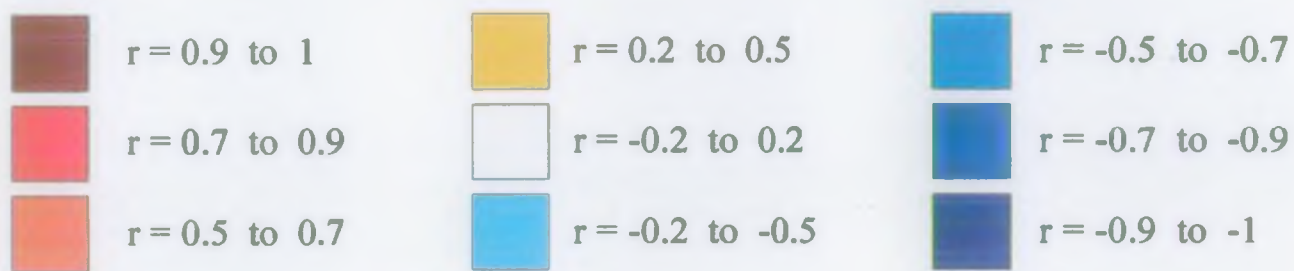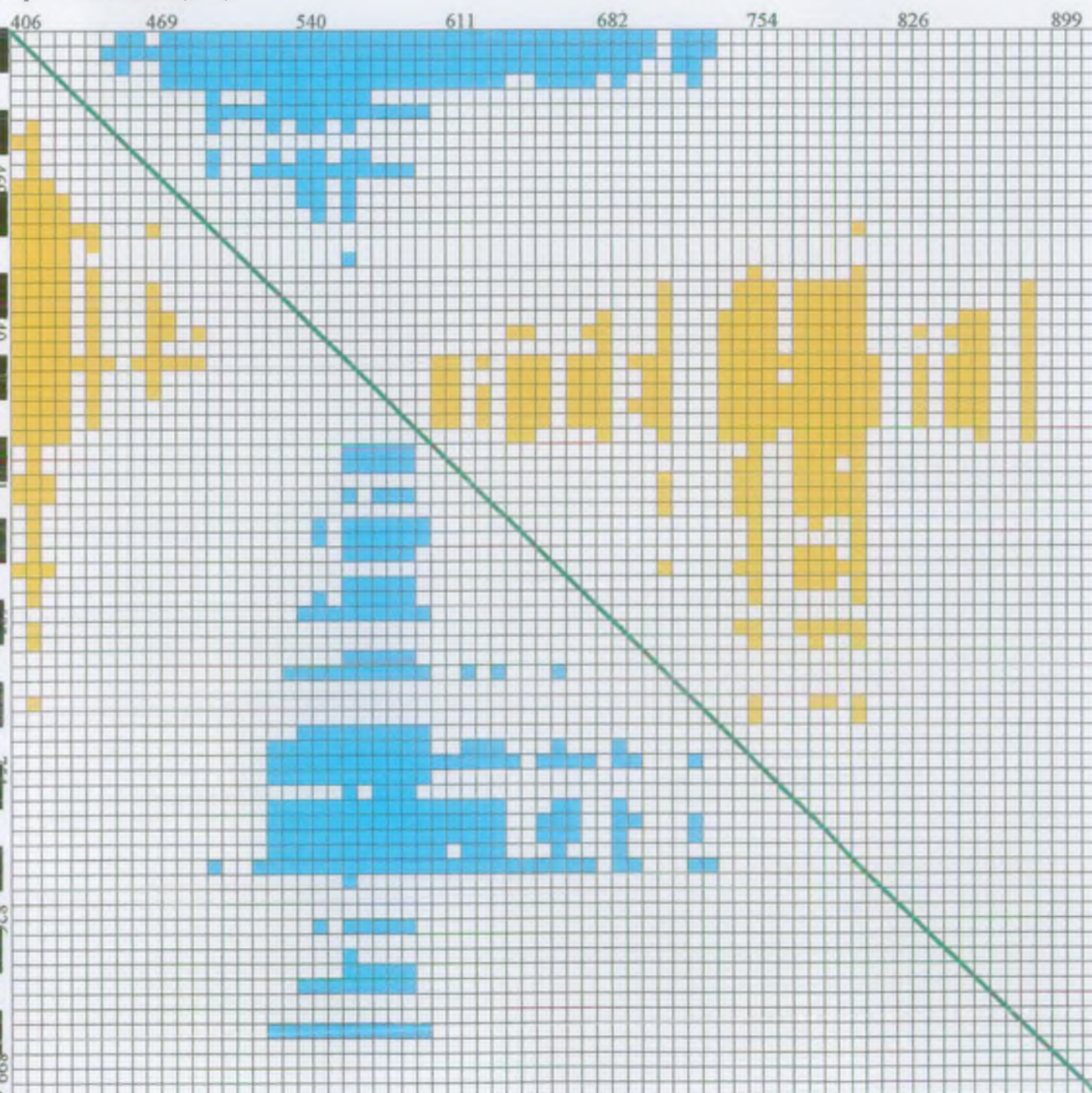
Figure 3. Correlation coefficient matrix for ratios of each band of enhanced spectral CASI image IMAG1877 compared with calibrated turbidity ground truth data from boat.
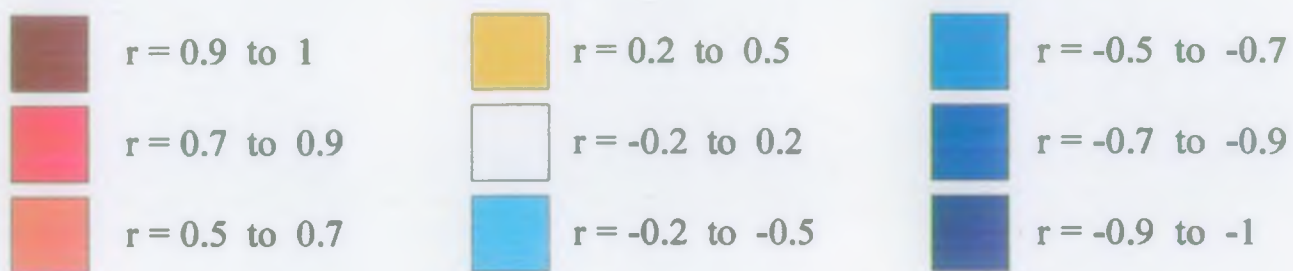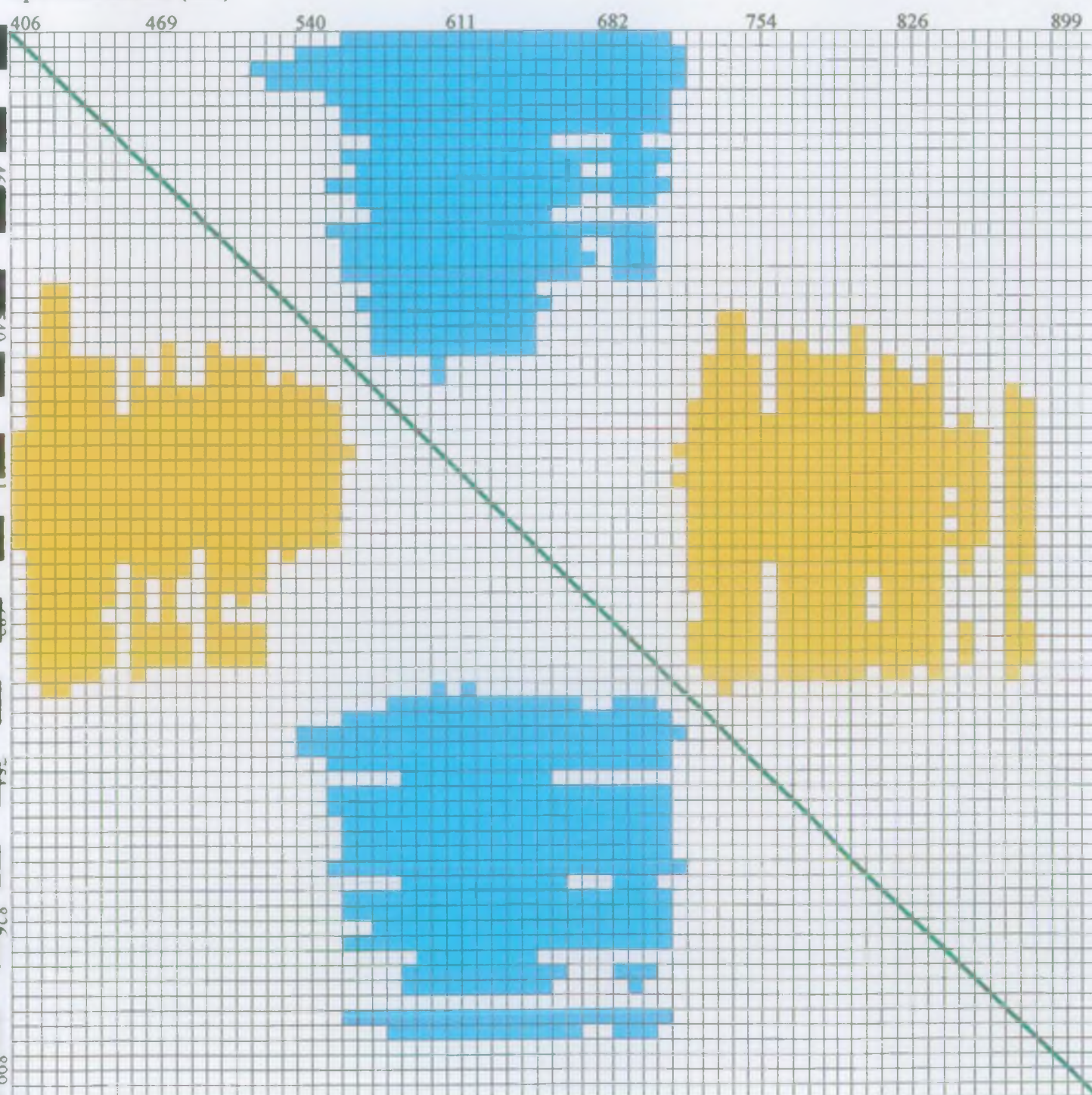
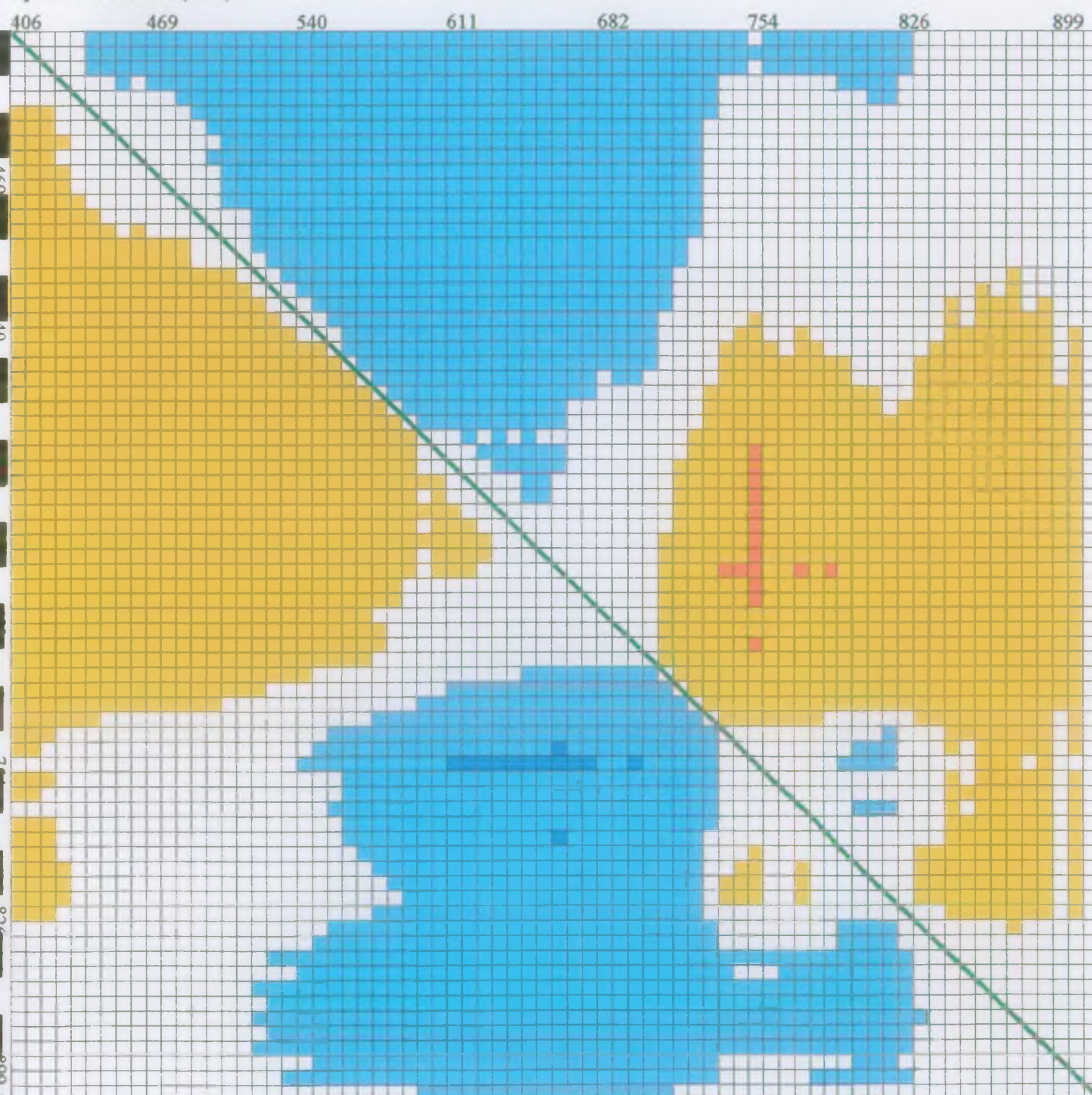Figure 4. Correlation coefficient matrix for ratios of each band of enhanced spectral CASI image IMAG2061 compared with calibrated transmission ground truth data from boat.

Figure 5. Correlation coefficient matrix for ratios of each band of enhanced spectral CASI image IMAG2062 compared with calibrated transmission ground truth data from boat.
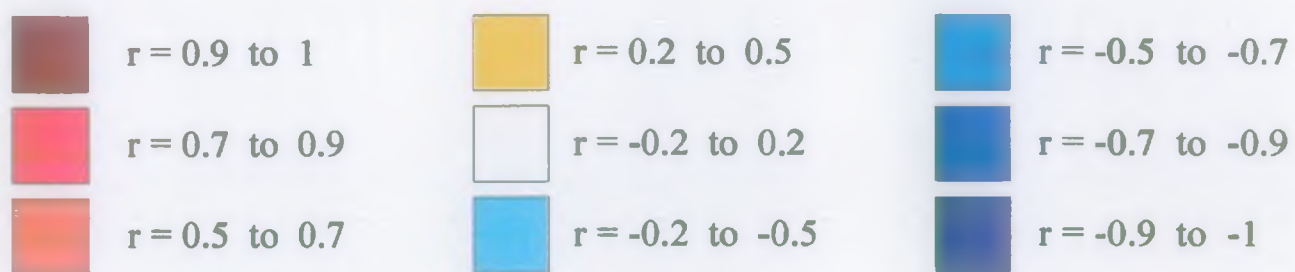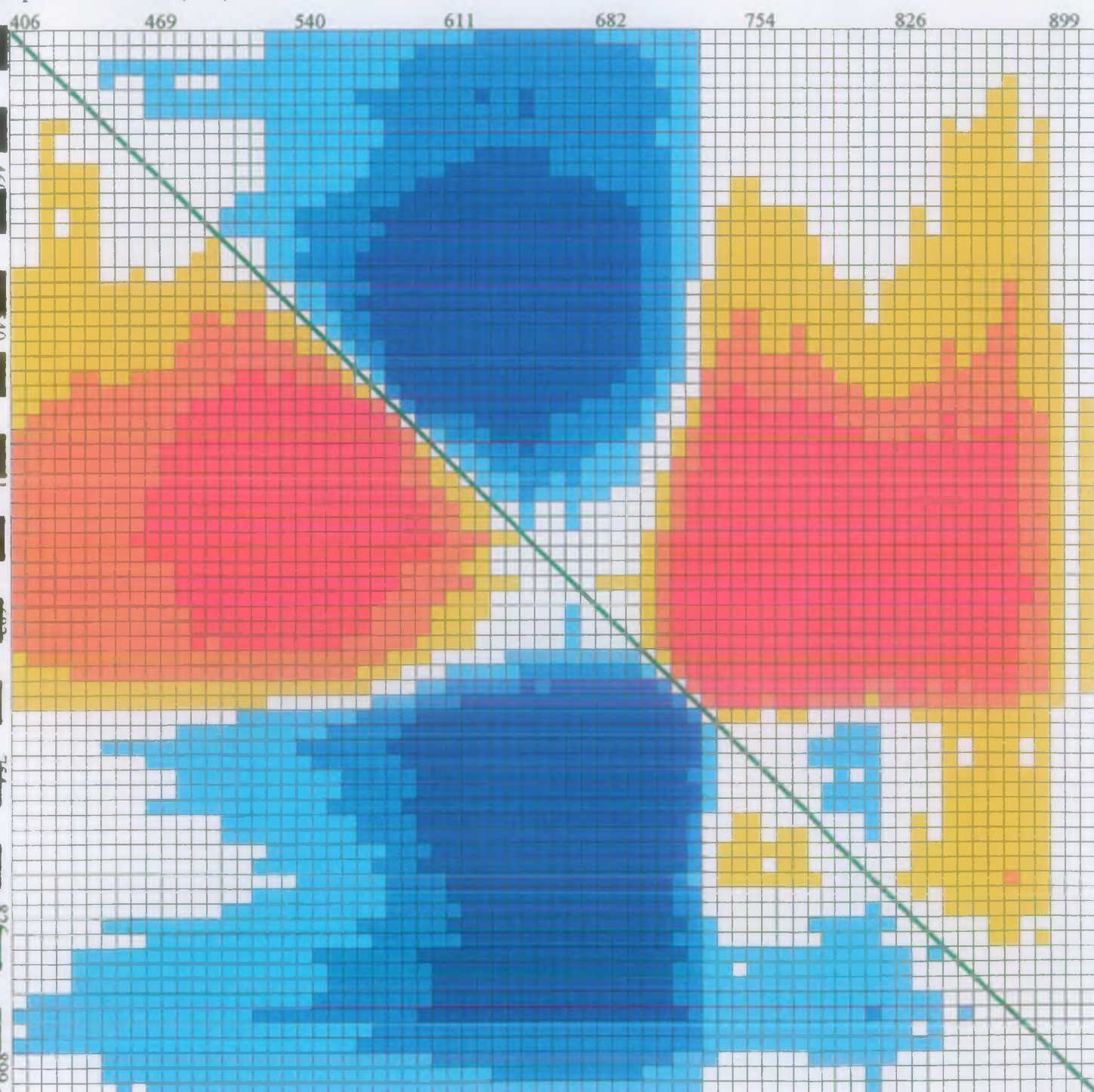
Figure 6. Correlation coefficient matrix for ratios of each band of enhanced spectral CASI image IMAG2356 compared with calibrated transmission ground truth data from boat.
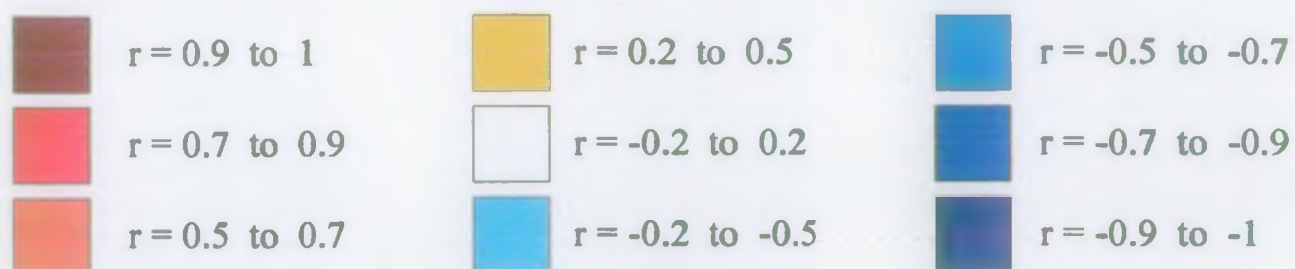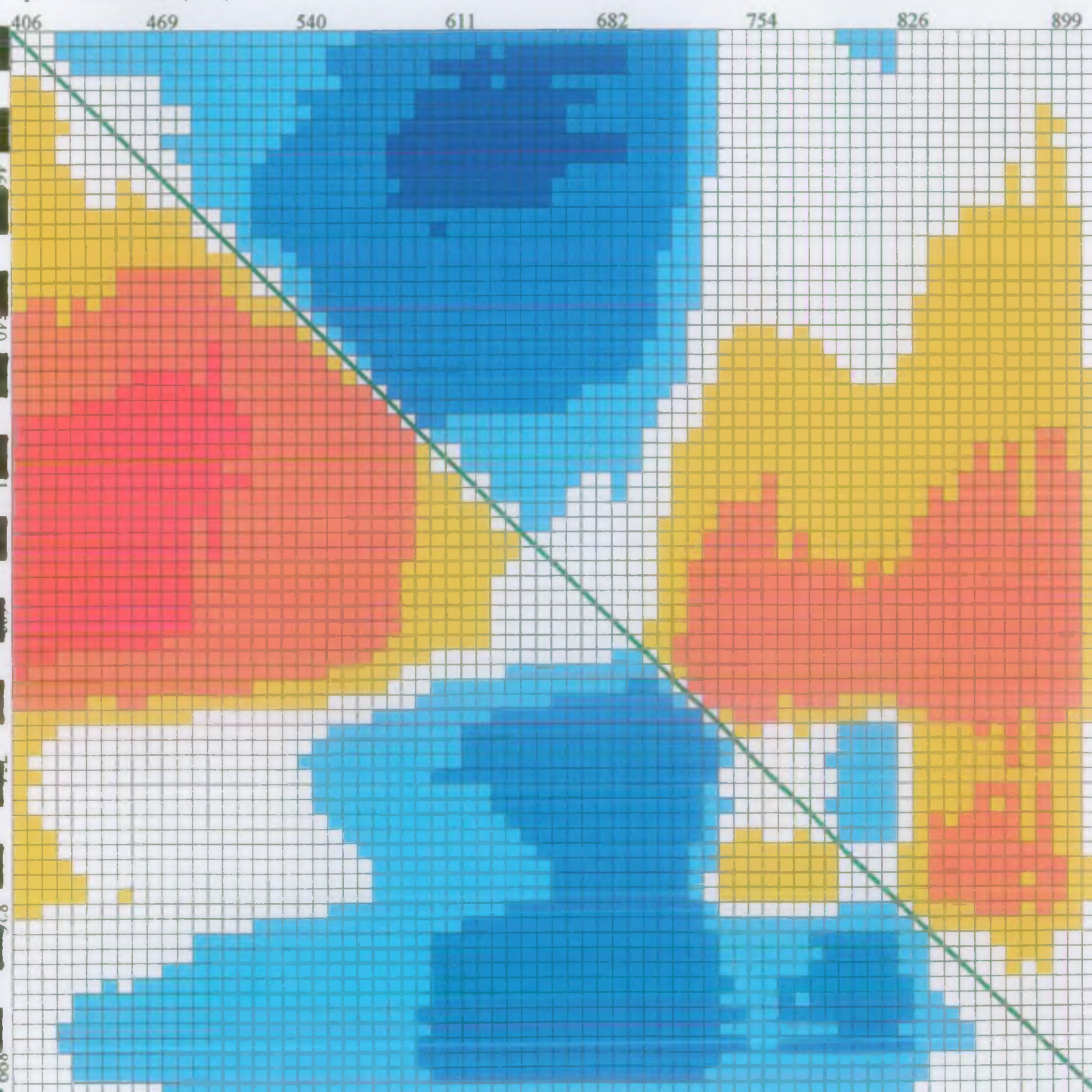
Figure 7. Correlation coefficient matrix for ratios of each band of enhanced spectral CASI image IMAG2357 compared with calibrated transmission ground truth data from boat.
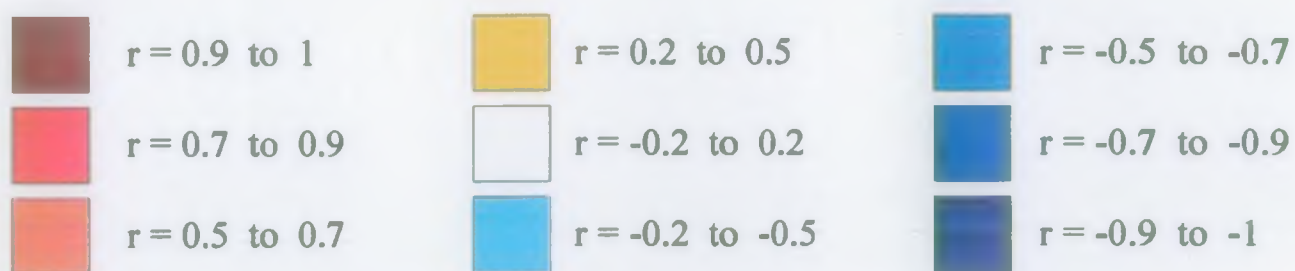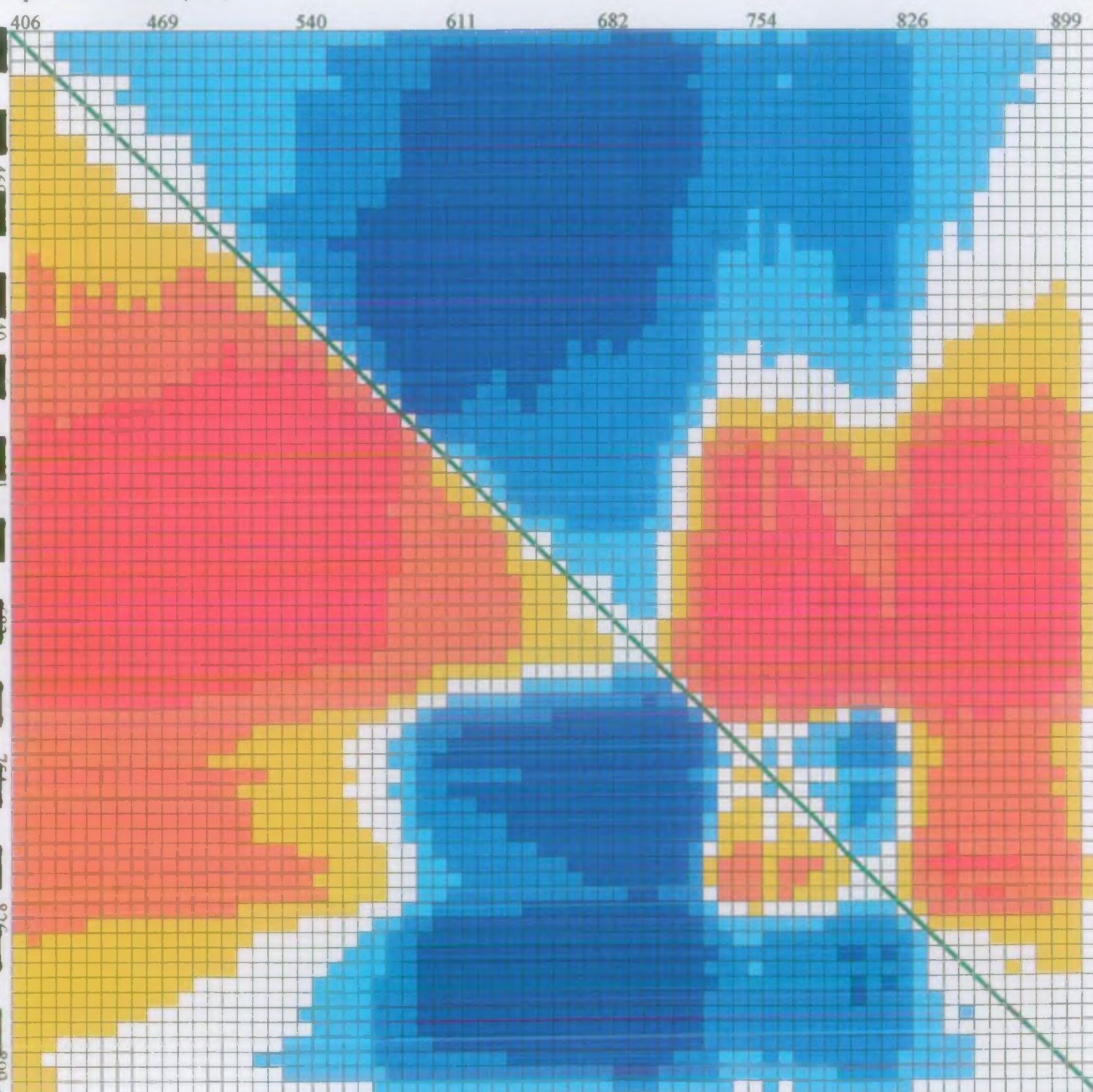
Figure 8. Correlation coefficient matrix for ratios of each band of enhanced spectral CASI image IMAG2369 compared with calibrated transmission ground truth data from boat.

Legend:
- r = 0.9 to 1
- r = 0.7 to 0.9
- r = 0.5 to 0.7
- r = 0.2 to 0.5
- r = -0.2 to 0.2
- r = -0.2 to -0.5
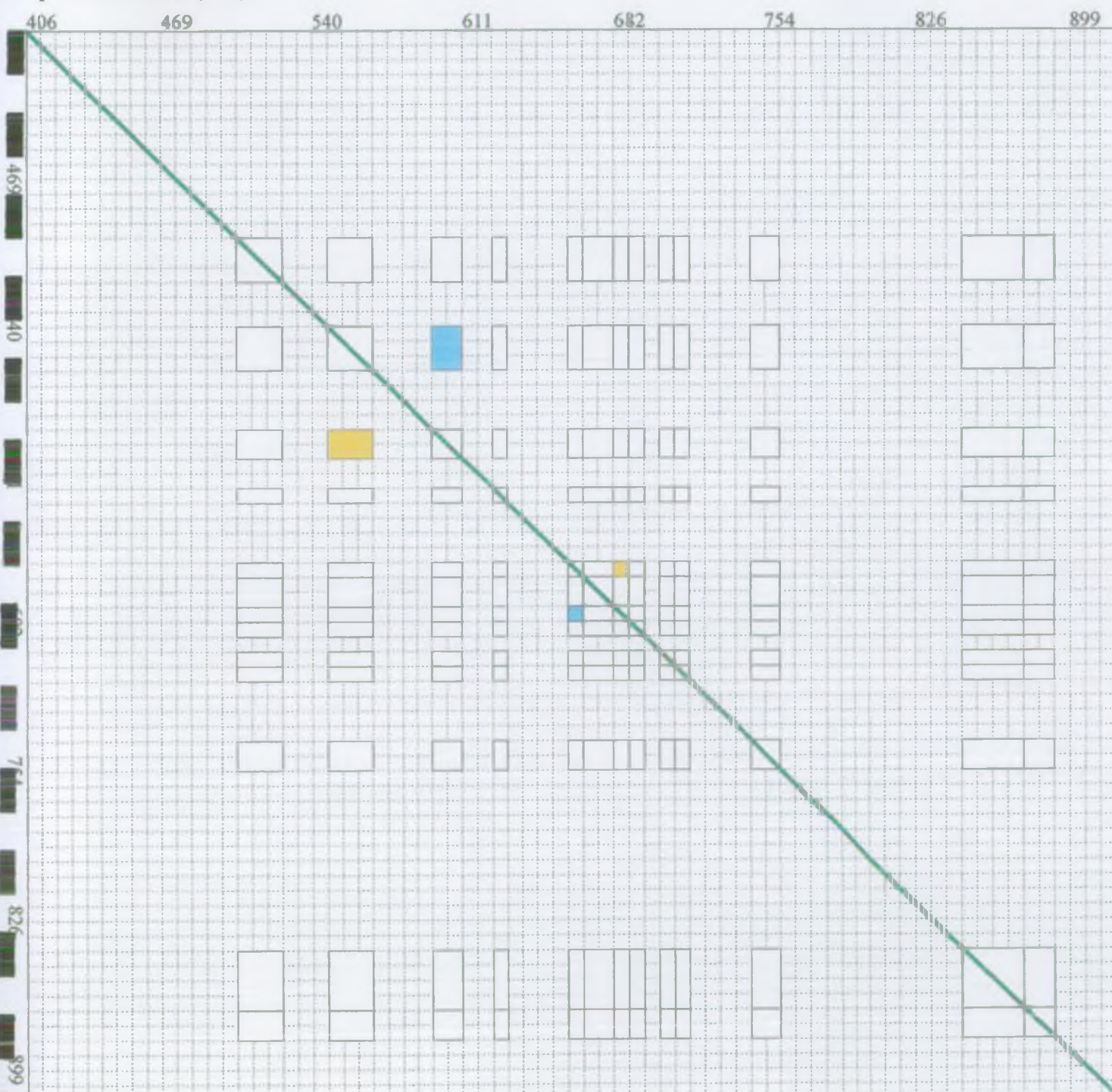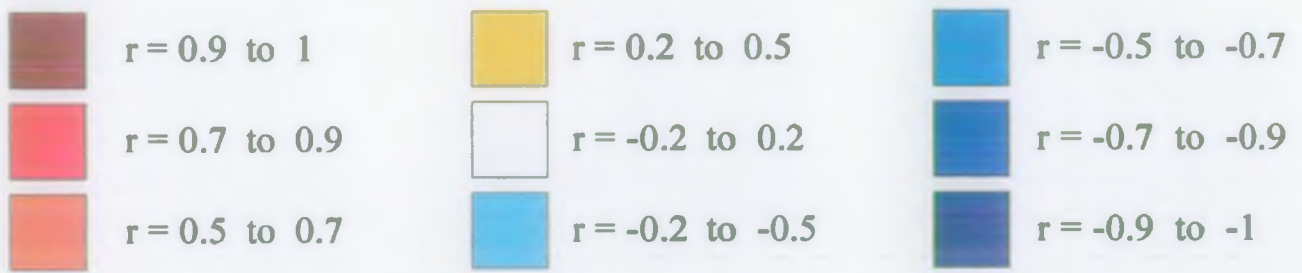- r = -0.5 to -0.7
- r = -0.7 to -0.9
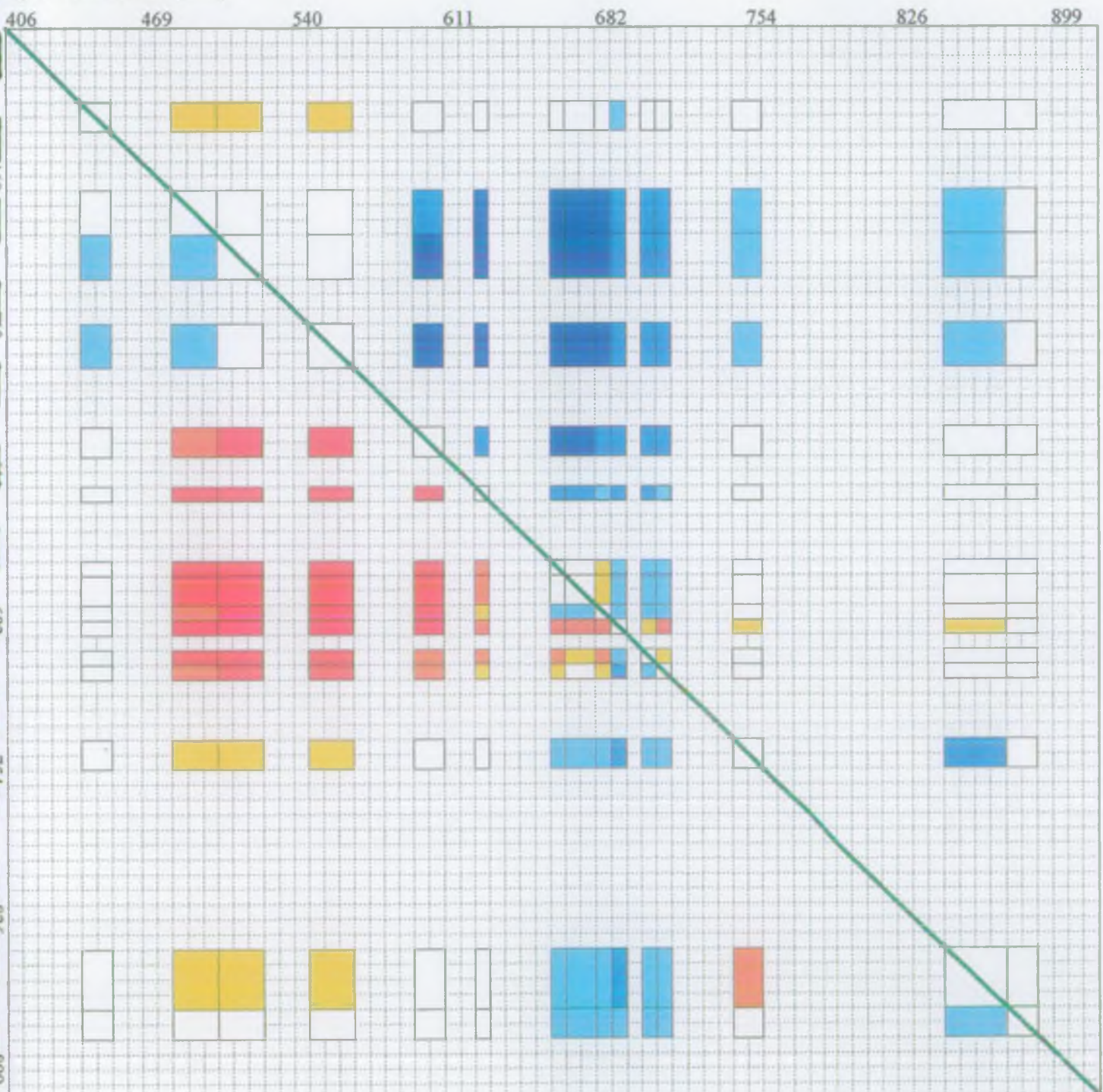- r = -0.9 to -1
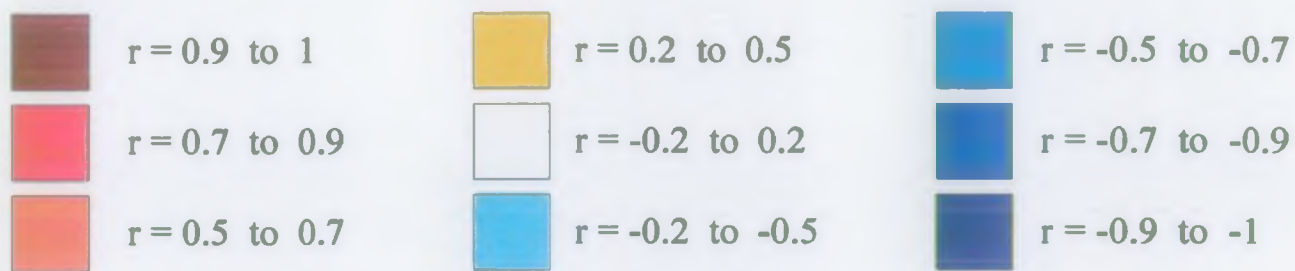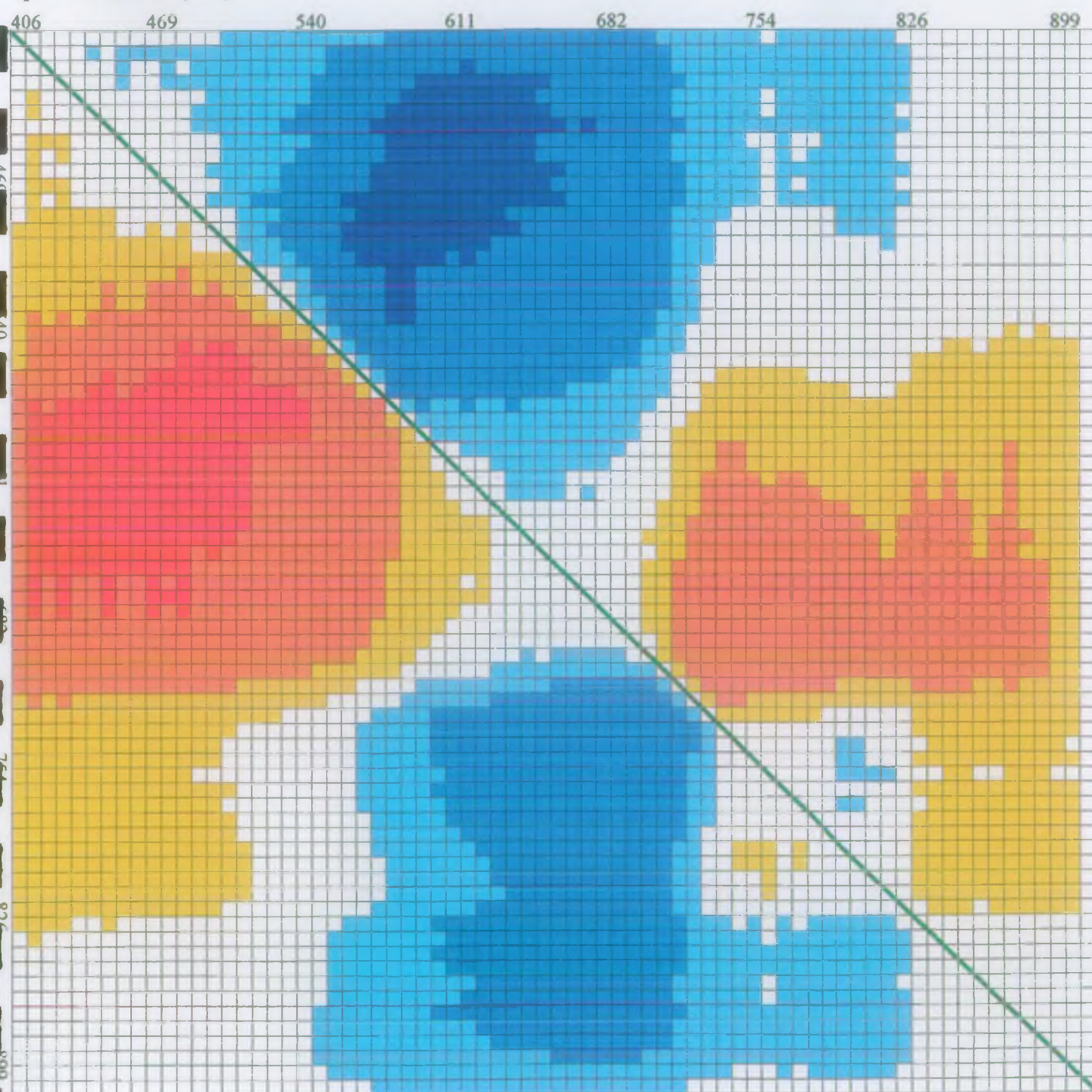
Spectral Band (nm)

Figure 9. Correlation coefficient matrix for ratios of each band of enhanced spectral CASI image IMAG2370 compared with calibrated transmission ground truth data from boat.
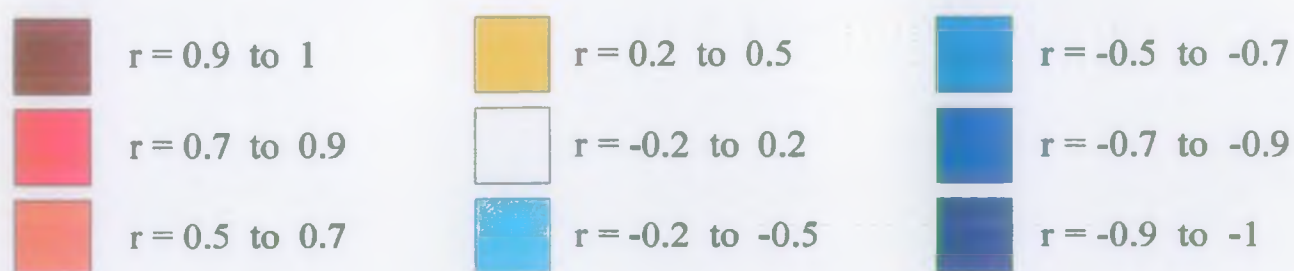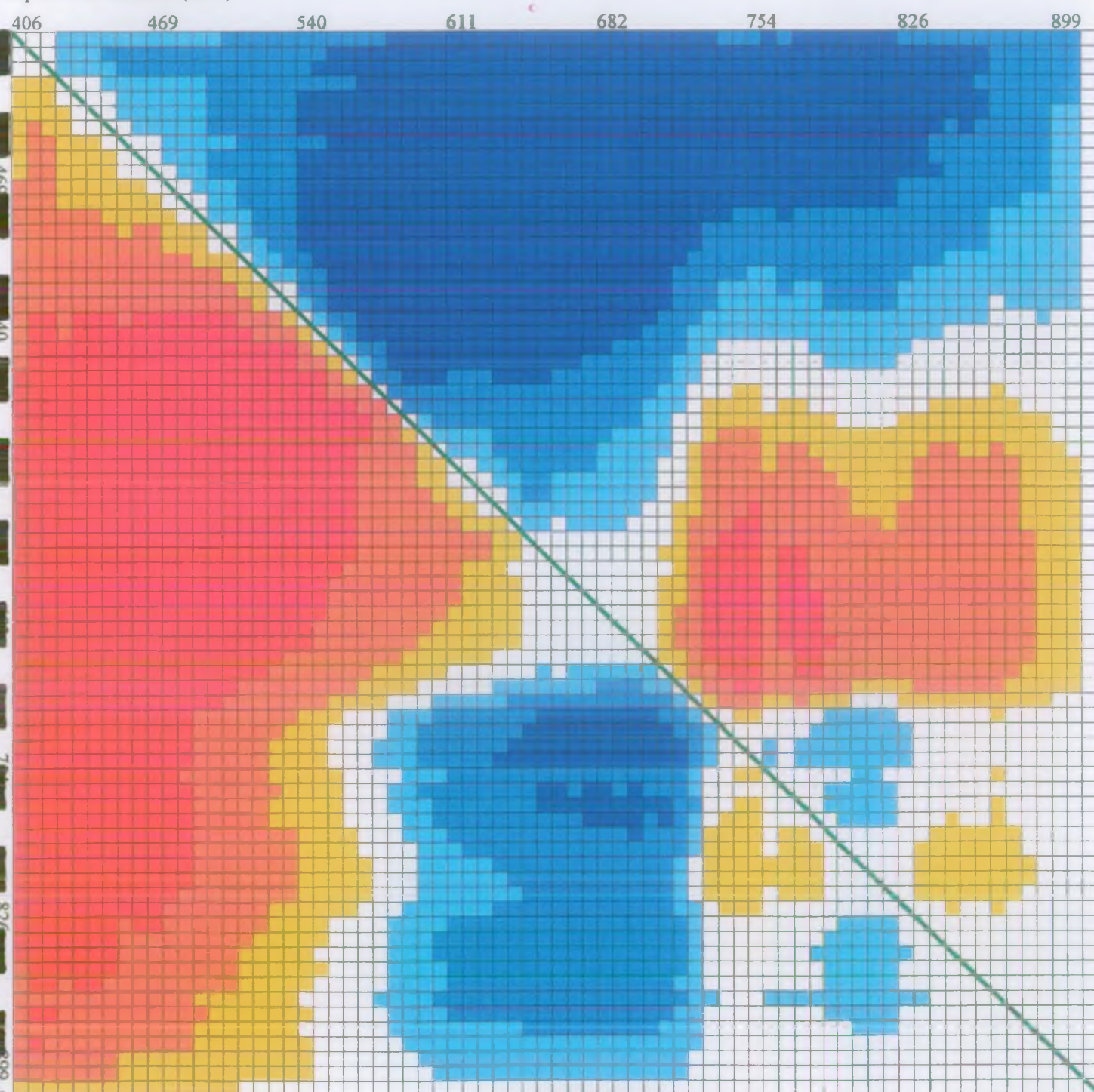
Figure 10. Averaged correlation coefficient matrix for ratios of all Bristol Channel enhanced spectral CASI images compared with calibrated transmission ground truth data from boat.
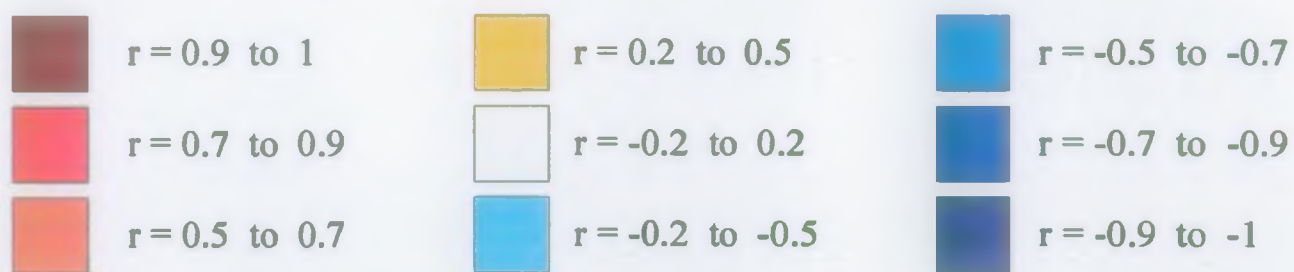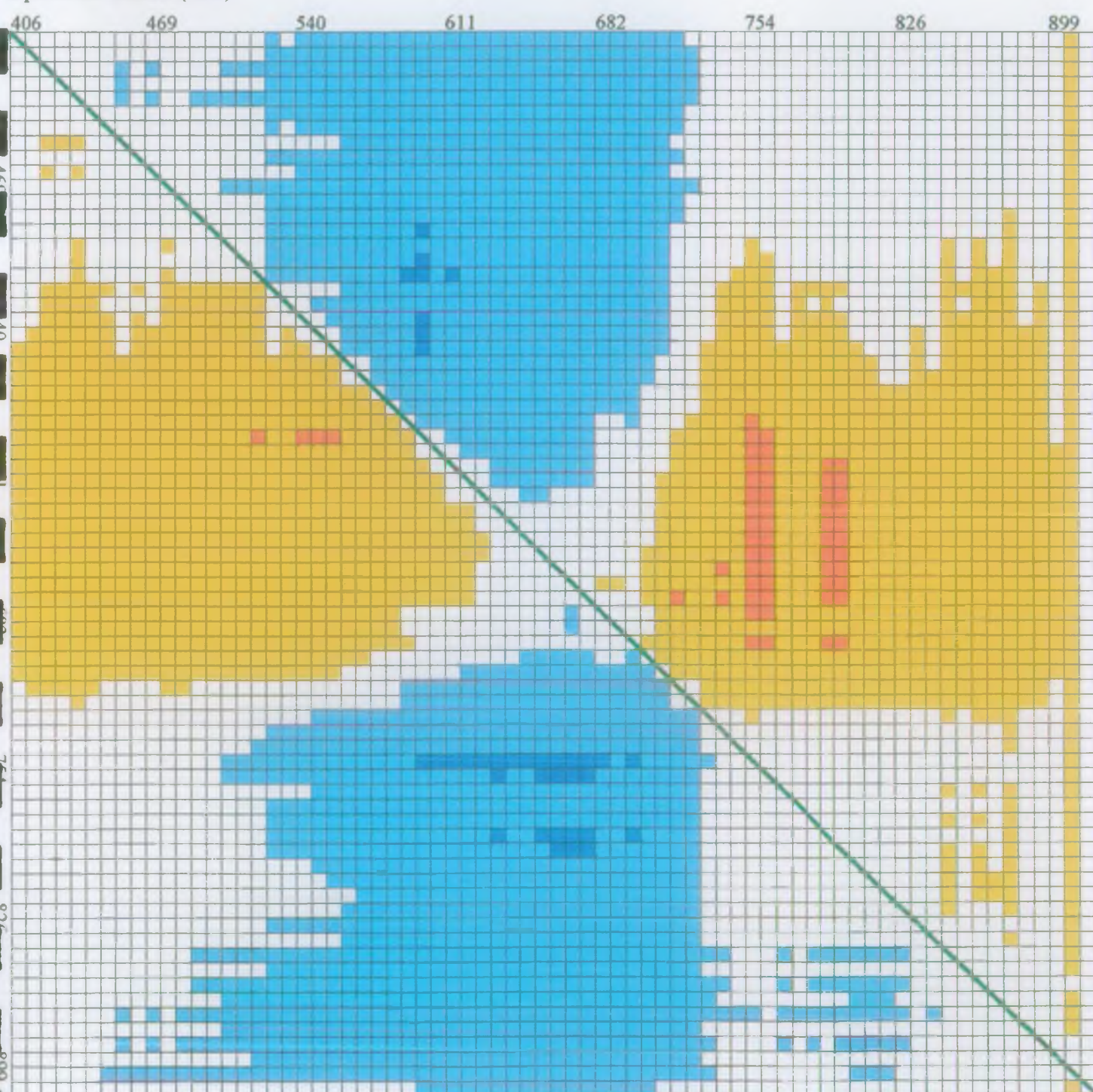
Figure 11. Averaged correlation coefficient matrix for ratios of two Holderness Coast enhanced spectral CASI images compared with calibrated transmission ground truth data from boat.
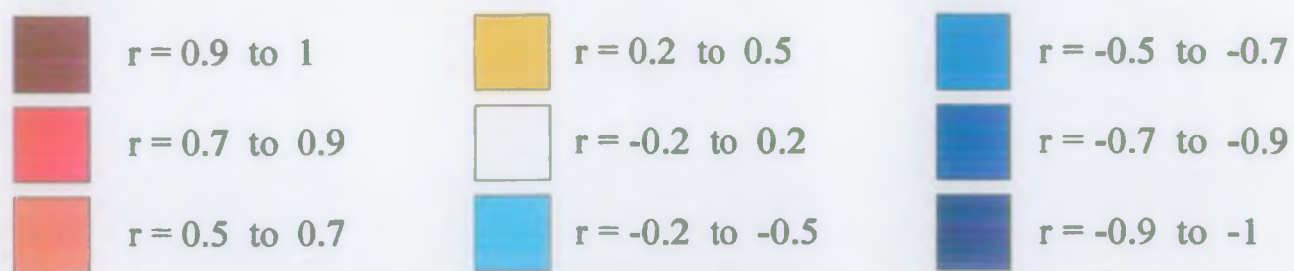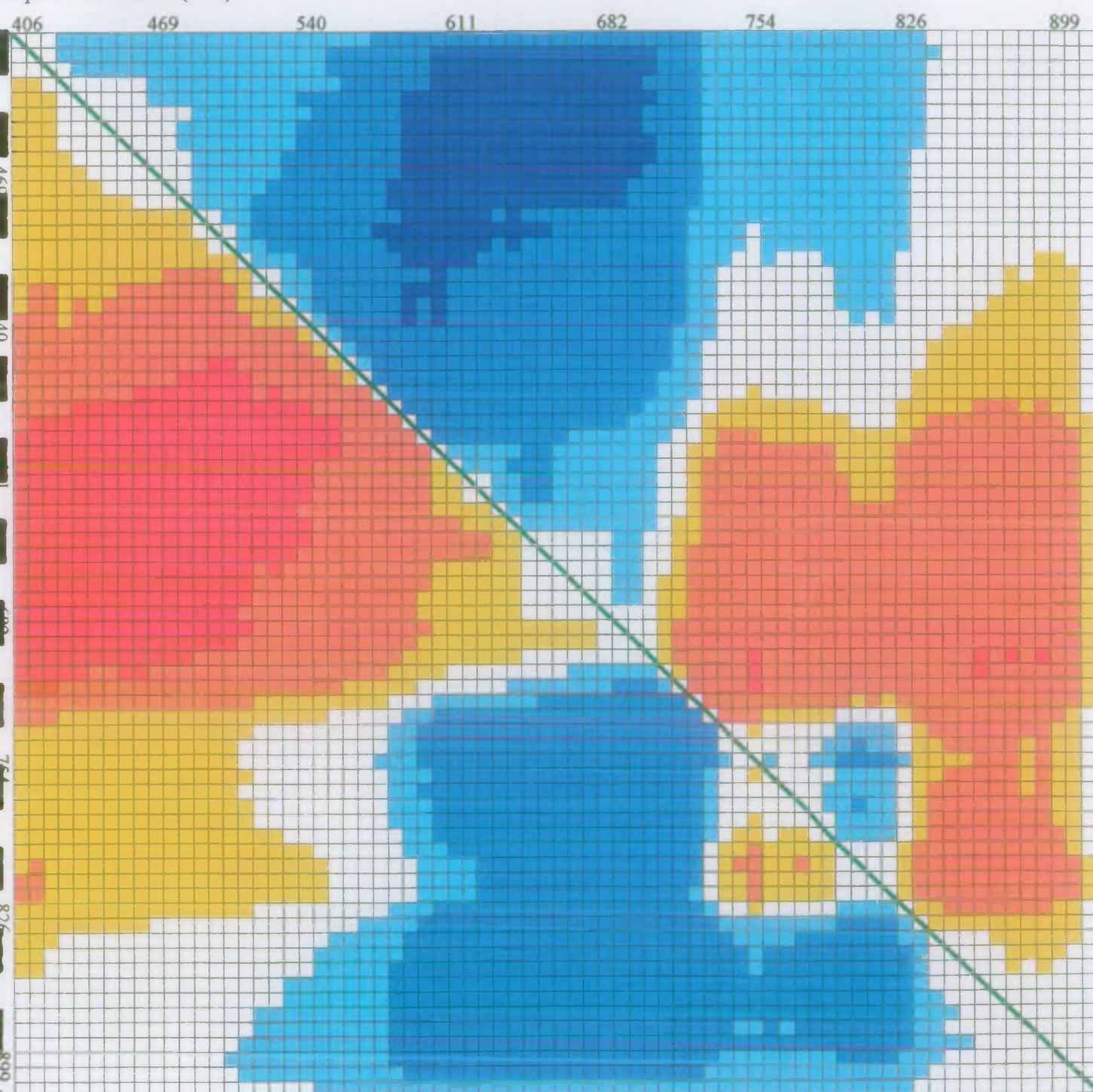
Figure 12. Averaged correlation coefficient matrix for ratios of all Holderness Coast enhanced spectral CASI images compared with calibrated transmission ground truth data from boat.

r = 0.9 to 1

r = 0.7 to 0.9

r = 0.5 to 0.7

r = 0.2 to 0.5

r = -0.2 to 0.2

r = -0.2 to -0.5

r = -0.5 to -0.7

r = -0.7 to -0.9

r = -0.9 to -1
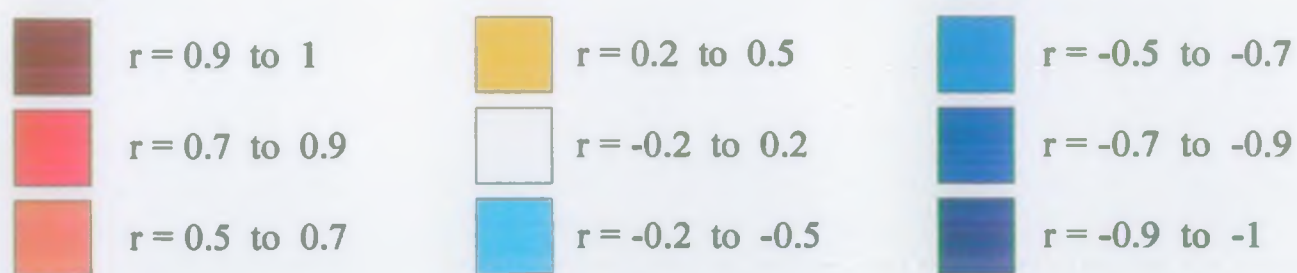
Spectral Band (nm)

Figure 13. Averaged correlation coefficient matrix for ratios of all Norfolk Coast enhanced spectral CASI images compared with calibrated turbidity ground truth data from boat.

	r = 0.9 to 1		r = 0.2 to 0.5		r = -0.5 to -0.7
	r = 0.7 to 0.9		r = -0.2 to 0.2		r = -0.7 to -0.9
	r = 0.5 to 0.7		r = -0.2 to -0.5		r = -0.9 to -1
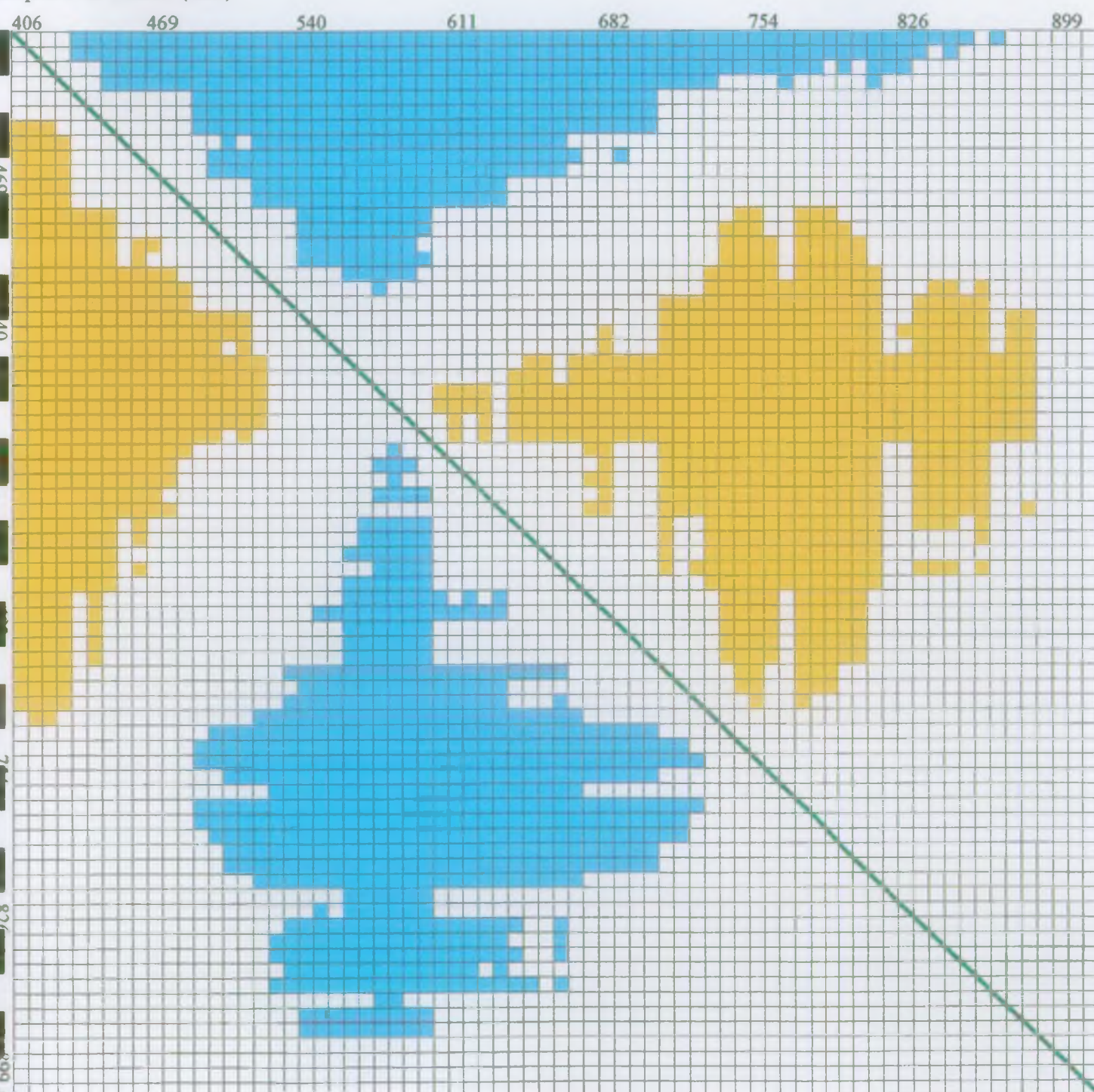
Spectral Band (nm)

Figure 14. Averaged correlation coefficient matrix for ratios of all All Sites (Global) enhanced spectral CASI images compared with calibrated transmission ground truth data from boat.
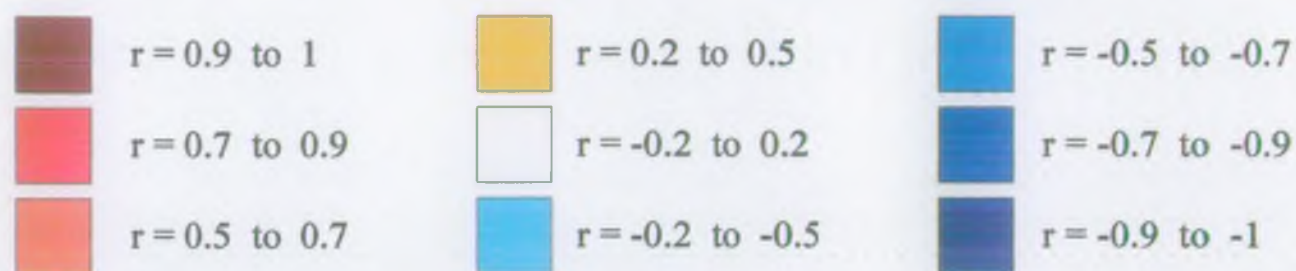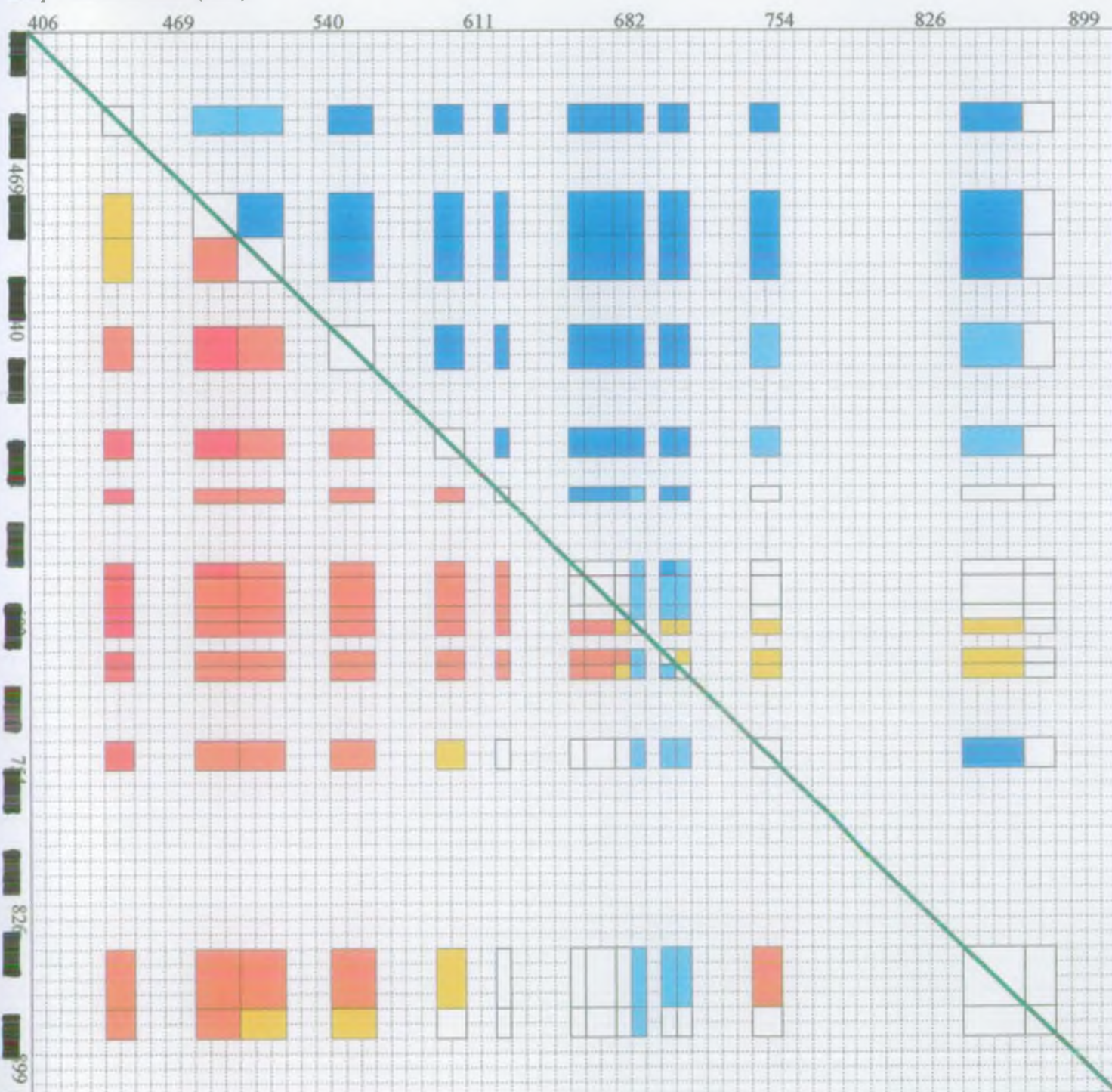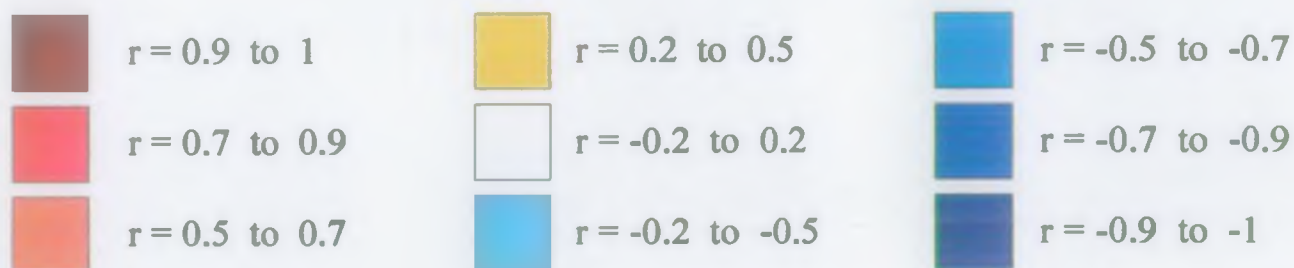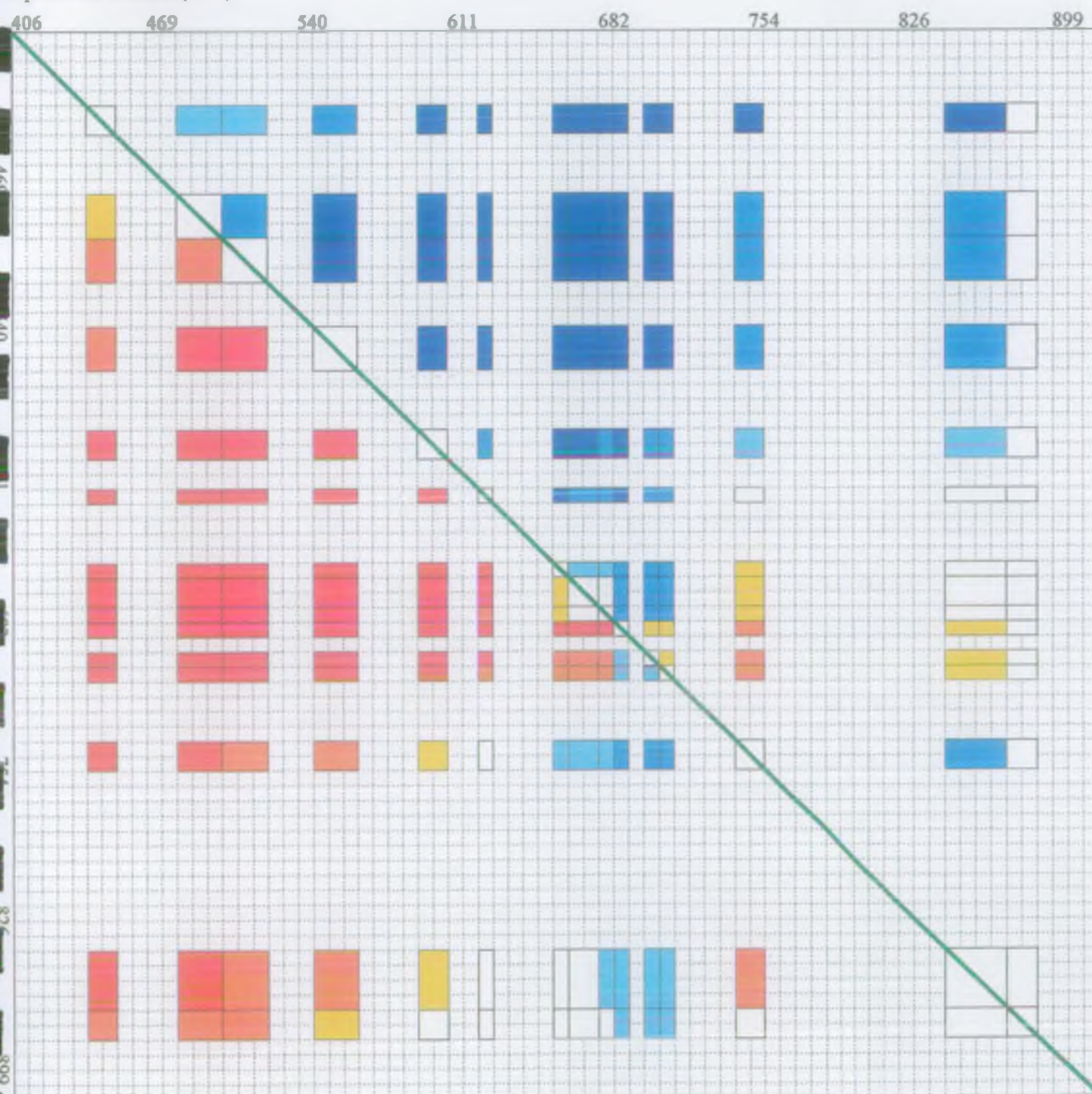
Figure 15. Correlation coefficient matrix for ratios of each band of atmospherically corrected CASI image IMAG1875 compared with calibrated turbidity ground truth data from boat.
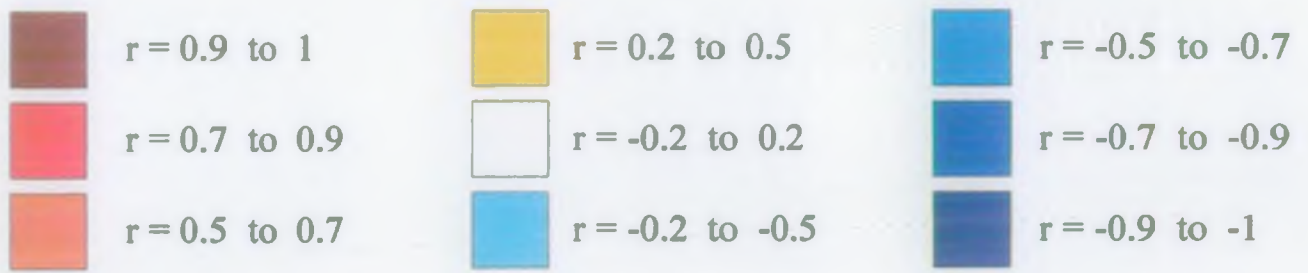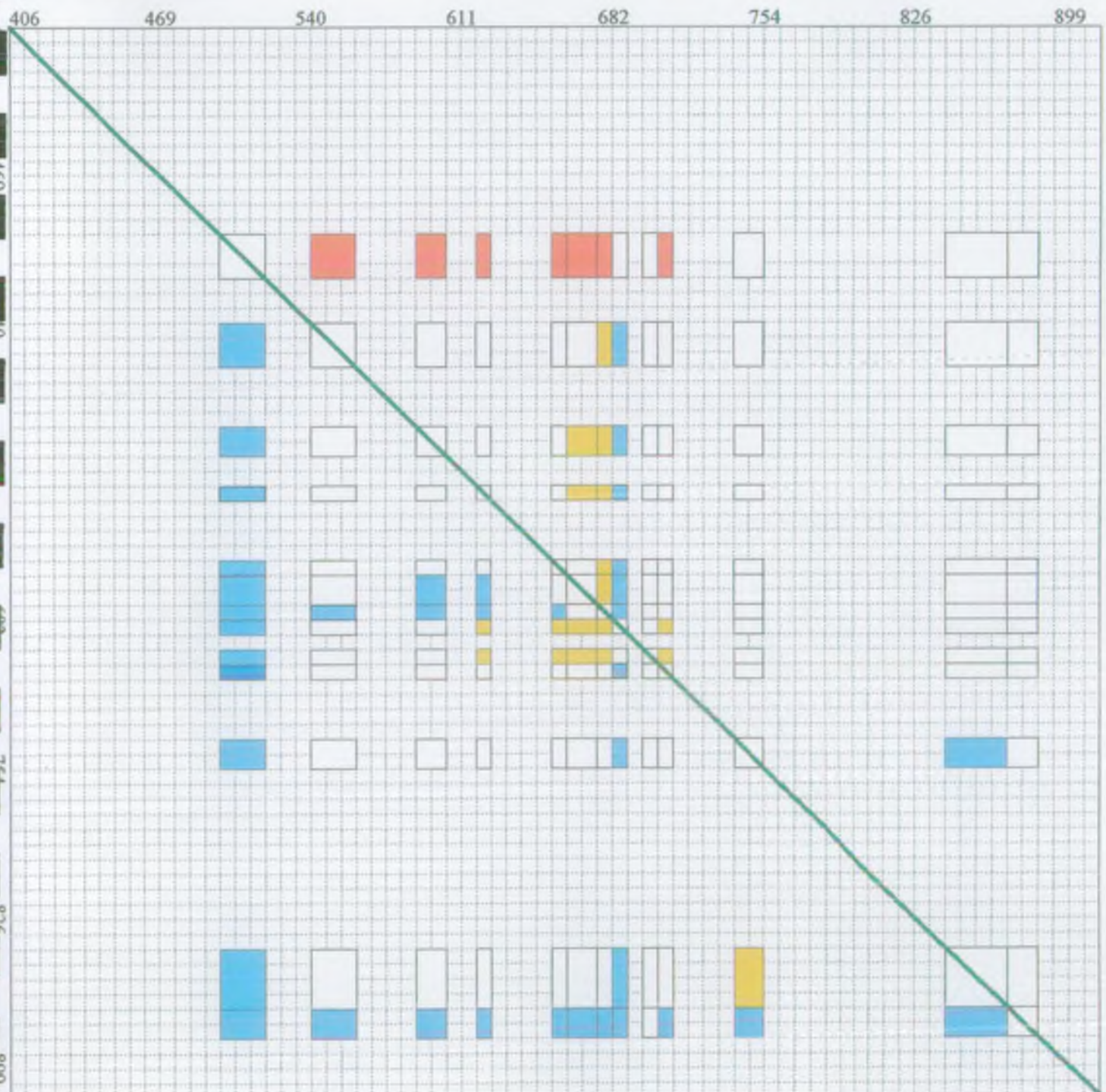
Figure 16. Correlation coefficient matrix for ratios of each band of atmospherically corrected CASI image IMAG1877 compared with calibrated turbidity ground truth data from boat.
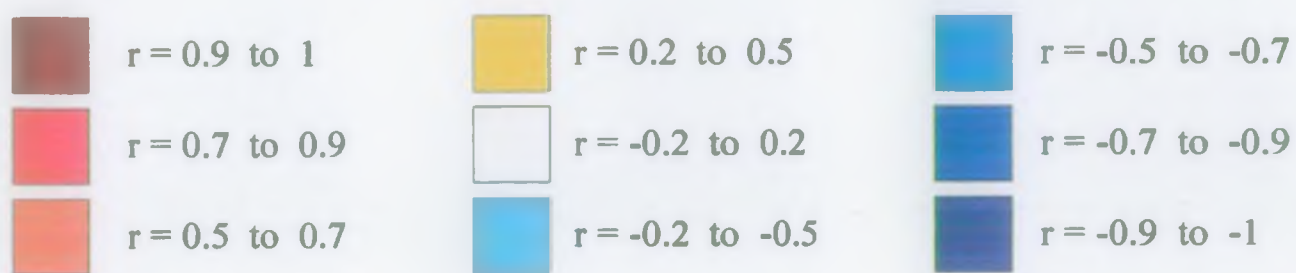
Figure 17. Correlation coefficient matrix for ratios of each band of atmospherically corrected CASI image IMAG2061 compared with calibrated transmission ground truth data from boat.

r = 0.9 to 1

r = 0.7 to 0.9

r = 0.5 to 0.7

r = 0.2 to 0.5

r = -0.2 to 0.2

r = -0.2 to -0.5

r = -0.5 to -0.7

r = -0.7 to -0.9

r = -0.9 to -1

Spectral Band (nm)

406   469   540   611   682   754   826   899

Figure 18. Correlation coefficient matrix for ratios of each band of atmospherically corrected CASI image IMAG2356 compared with calibrated transmission ground truth data from boat.
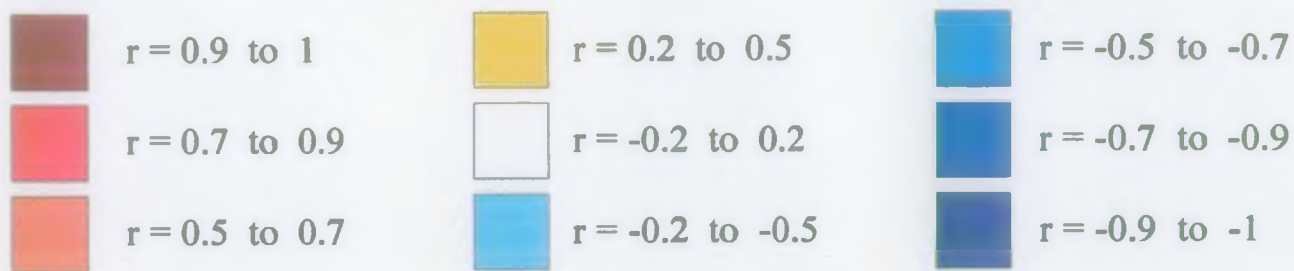
Figure 19. Correlation coefficient matrix for ratios of each band of atmospherically corrected CASI image IMAG2357 compared with calibrated transmission ground truth data from boat.

Figure 20. Correlation coefficient matrix for ratios of each band of atmospherically corrected CASI image IMAG2370 compared with calibrated transmission ground truth data from boat.
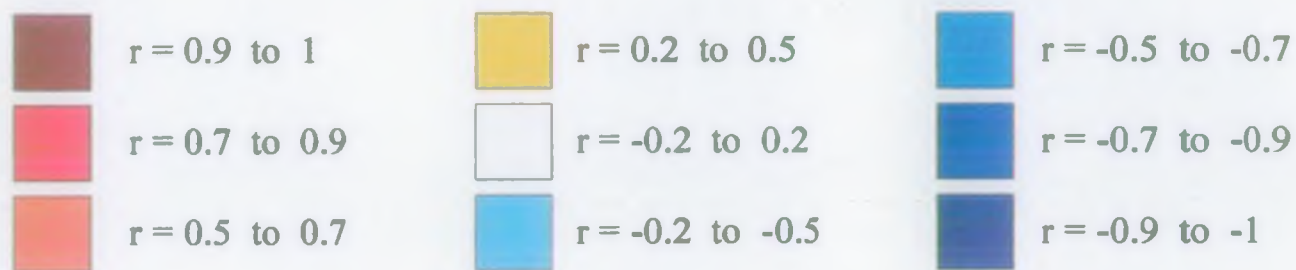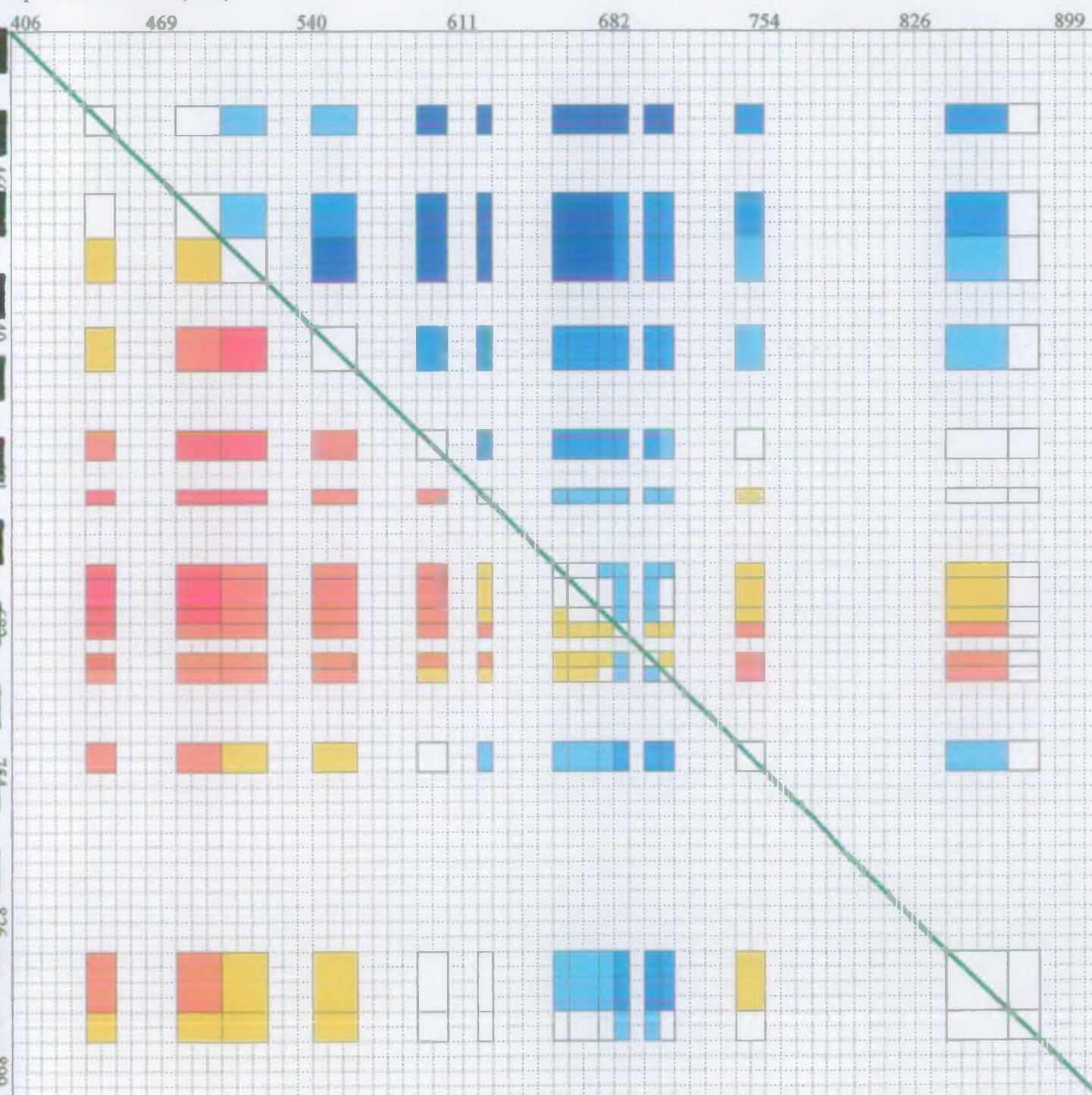
Figure 21. Non-Linear Regression Calibration Curve For Image 2061, Bristol Channel 24/06/96.

$$\frac{\text{ratio as}}{\text{SS@105 (mg/l)}} = \text{EXP}(a + (b * \text{ratio}))$$

$$a = -0.793$$
$$b = 0.929$$

Transmission Calibrated to mg/l of Suspended Solids at 105°C

Ratio of Band 33 / Band 50
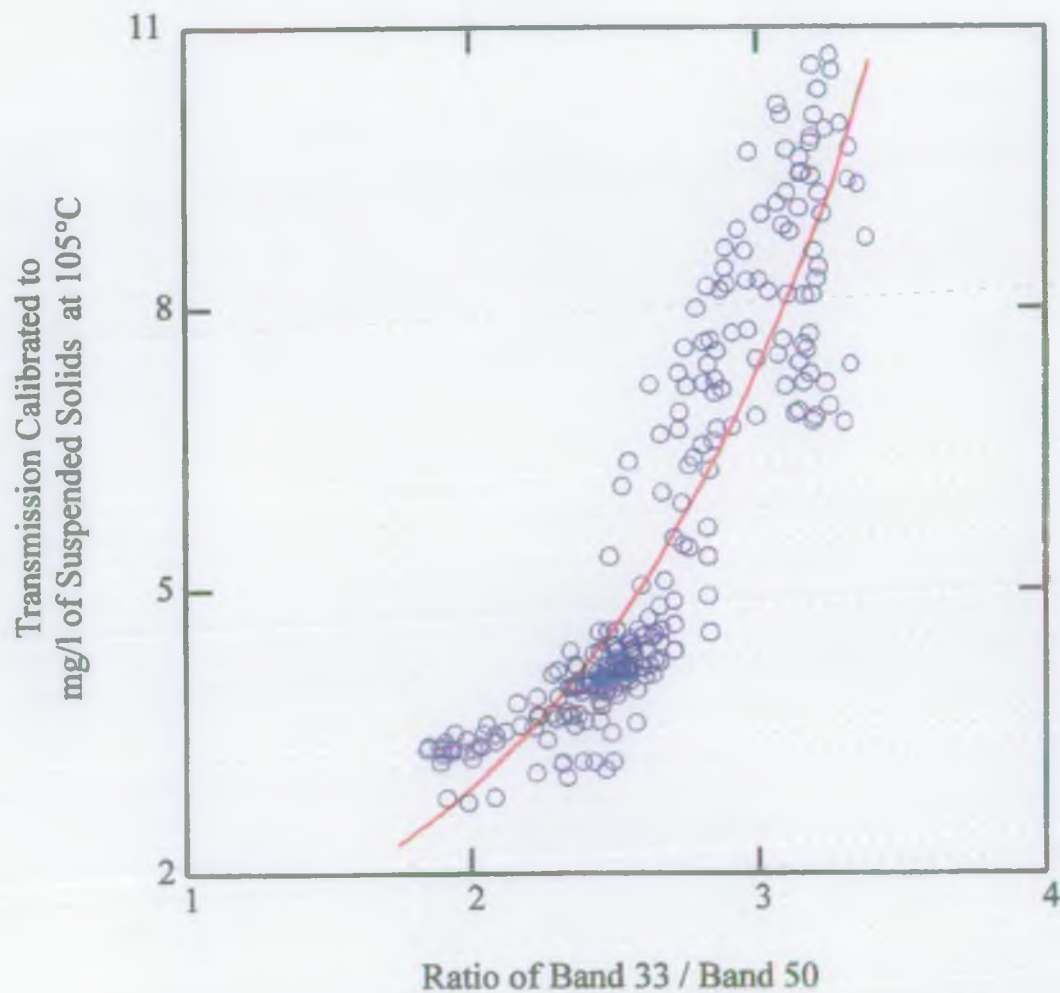
Figure 22. Non-Linear Regression Calibration Curve For Combined North Norfolk Images 1875, 1876 and 1877, 30/05/96.

$$\frac{\text{ratio as}}{\text{SS@105 (mg/l)}} = EXP(a + (b * ratio))$$

$$a = -5.920$$
$$b = 3.607$$

Ratio of Band 25 / Band 49
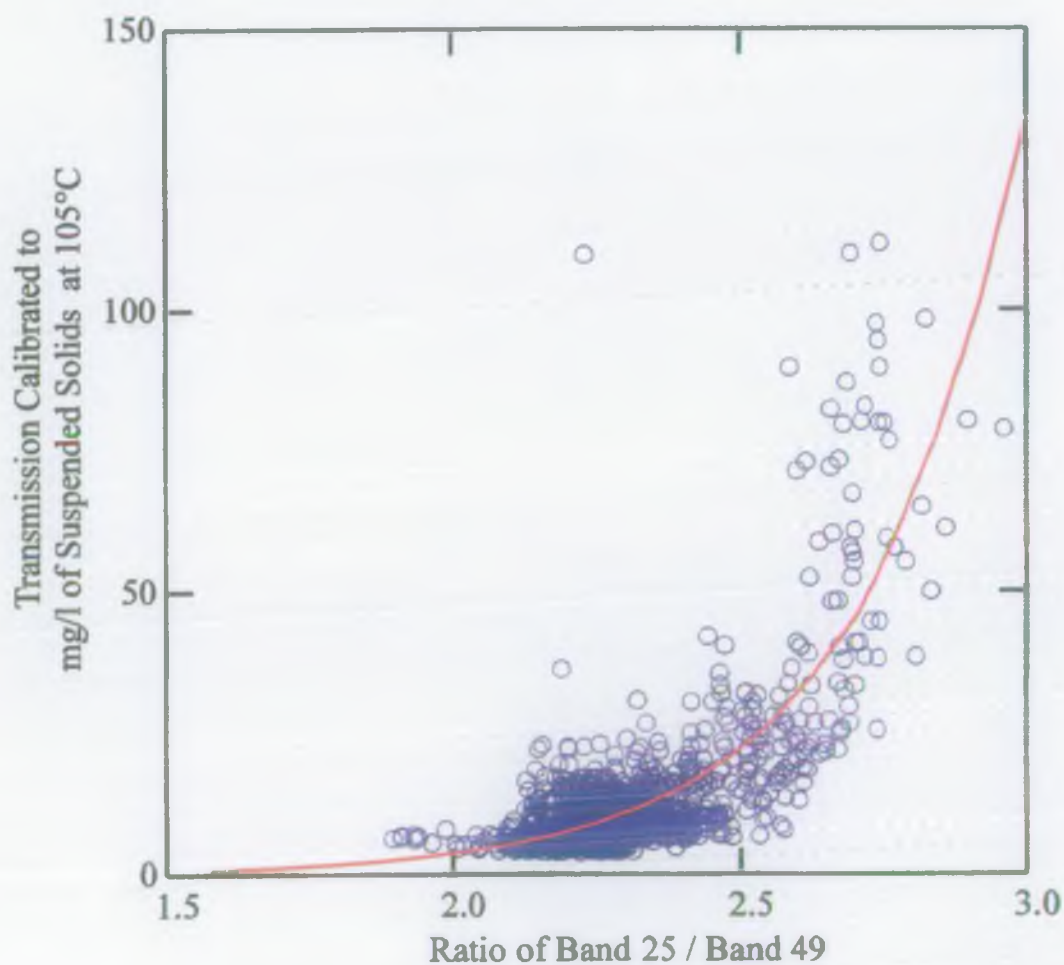
Figure 23. Non-Linear Regression Calibration Curve For Image 1875, North Norfolk 30/05/96.

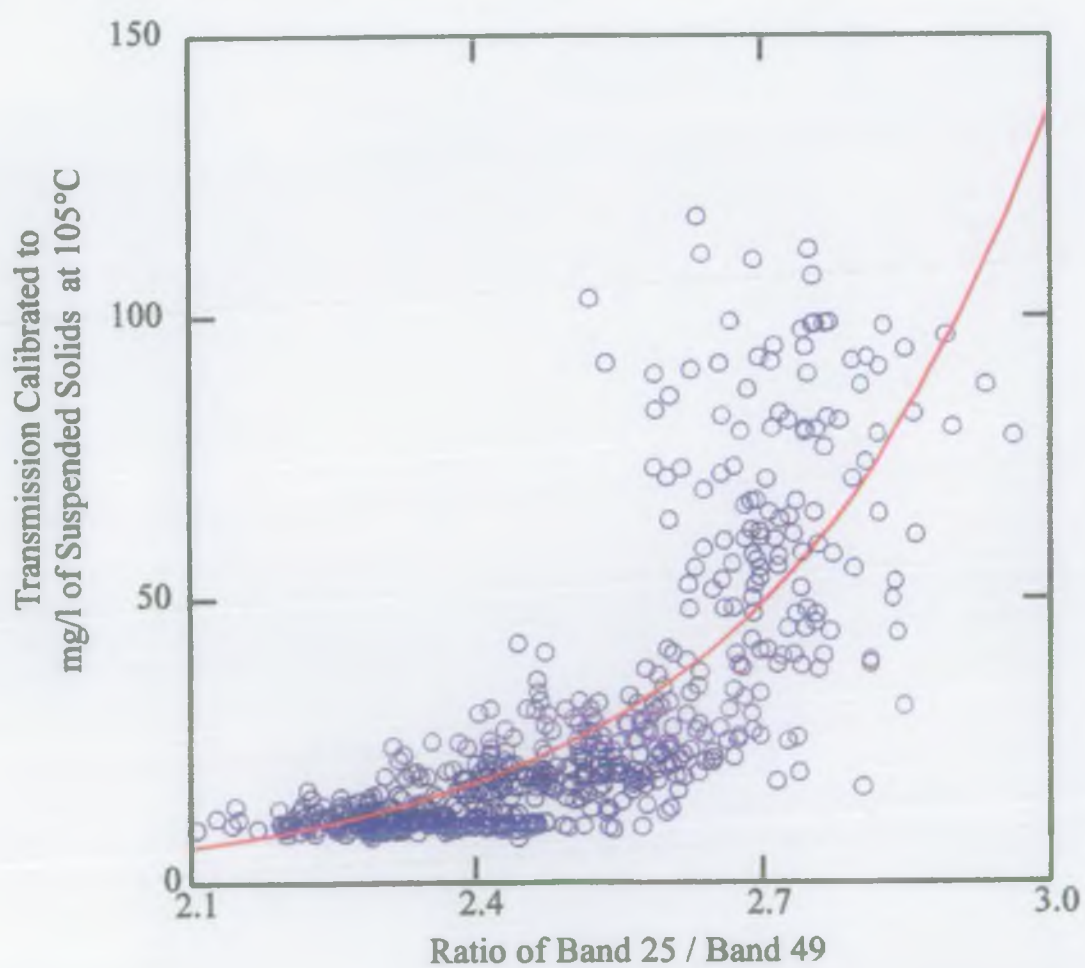$$\frac{\text{ratio as}}{\text{SS@105 (mg/l)}} = \text{EXP}(a + (b * \text{ratio}))$$

$$a = -5.356$$
$$b = 3.426$$

Transmission Calibrated to mg/l of Suspended Solids at 105°C

Ratio of Band 25 / Band 49

Figure 24. Comparison of Scatter Plots for Images 1875 (North Norfolk) and 2061 (Bristol Channel).

Y-axis: Transmission Calibrated to mg/l of Suspended Solids at 105°C

Norfolk Data (Image 1875)

Bristol Channel Data (Image 2061)

X-axis: Ratio of Band 28 / Band 50
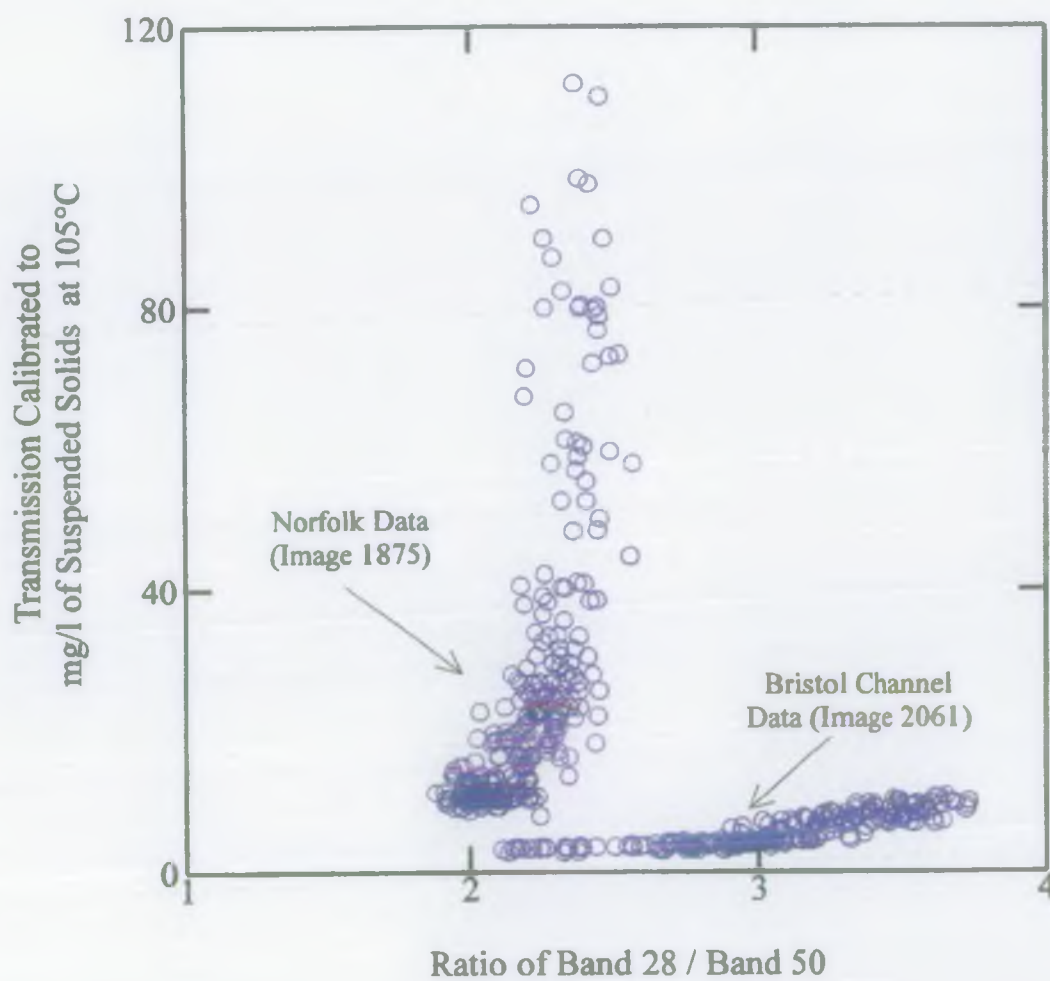
Figure 25. CASI Image 2061, Calibrated to Suspended Solids, Using Image Specific Linear Algorithm.
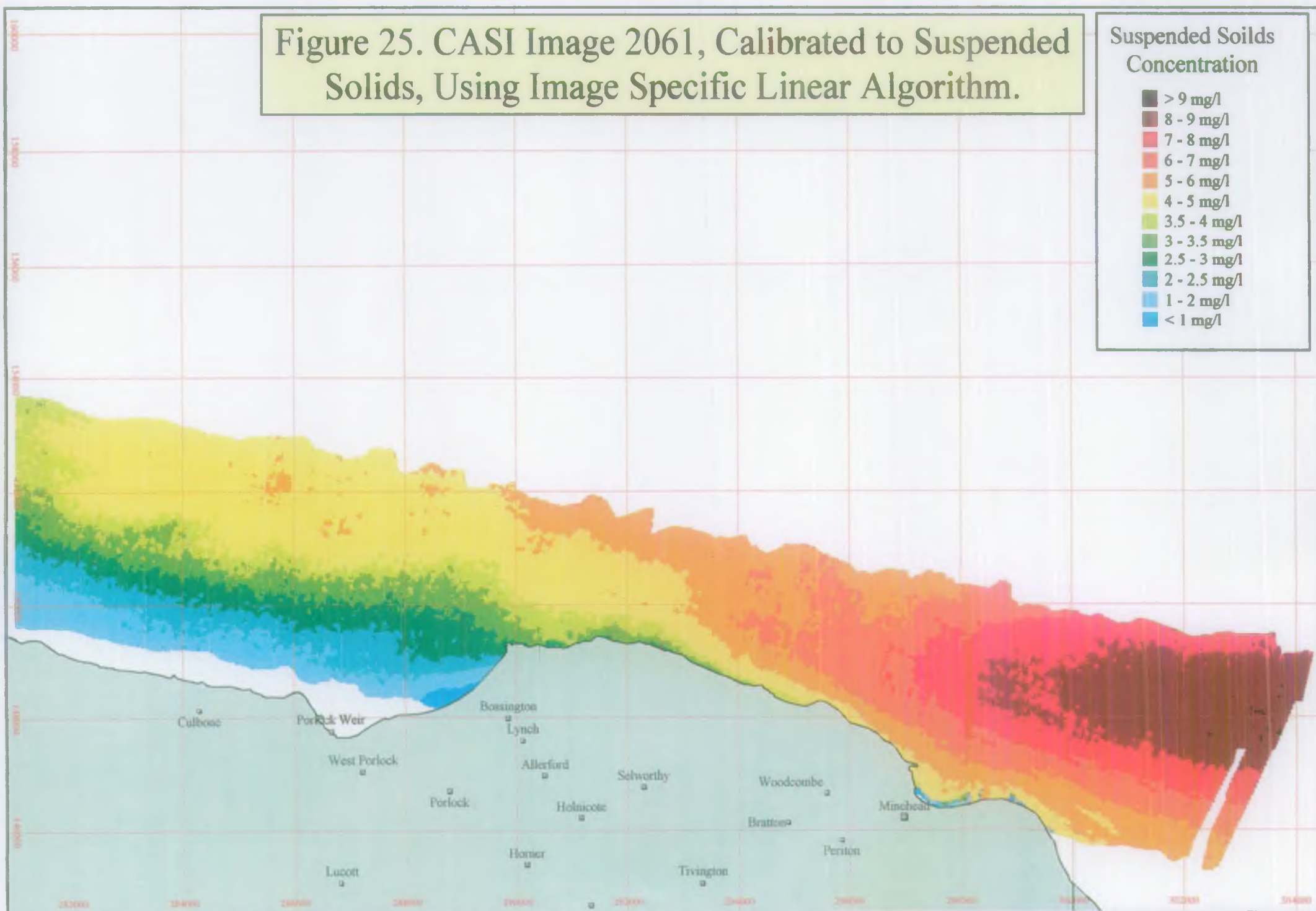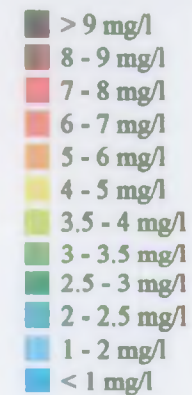
Figure 26. CASI Image 2061, Calibrated to Suspended Solids, Using Local (Bristol Channel) Linear Algorithm

Suspended Soilds Concentration
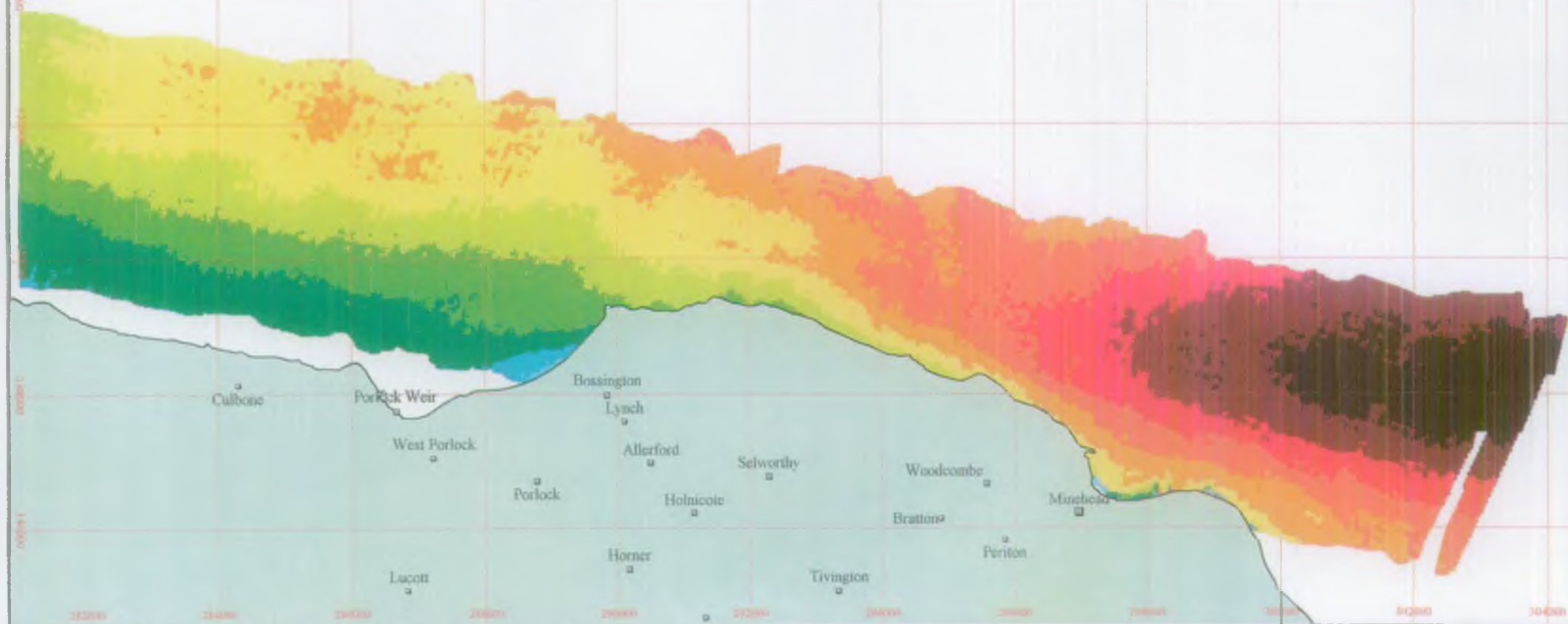
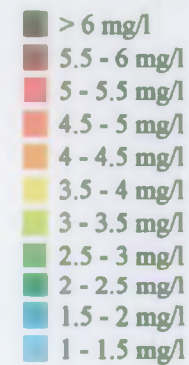- \> 6 mg/l
- 5.5 - 6 mg/l
- 5 - 5.5 mg/l
- 4.5 - 5 mg/l
- 4 - 4.5 mg/l
- 3.5 - 4 mg/l
- 3 - 3.5 mg/l
- 2.5 - 3 mg/l
- 2 - 2.5 mg/l
- 1.5 - 2 mg/l
- 1 - 1.5 mg/l

Figure 27. CASI Image 2061, Calibrated to Suspended Solids, Using Image Specific Exponential Algorithm

Suspended Soilds Concentration

- > 9 mg/l
- 8 - 9 mg/l
- 7 - 8 mg/l
- 6 - 7 mg/l
- 5.5 - 6 mg/l
- 4 - 4.5 mg/l
- 4.5 - 5 mg/l
- 4 - 4.5 mg/l
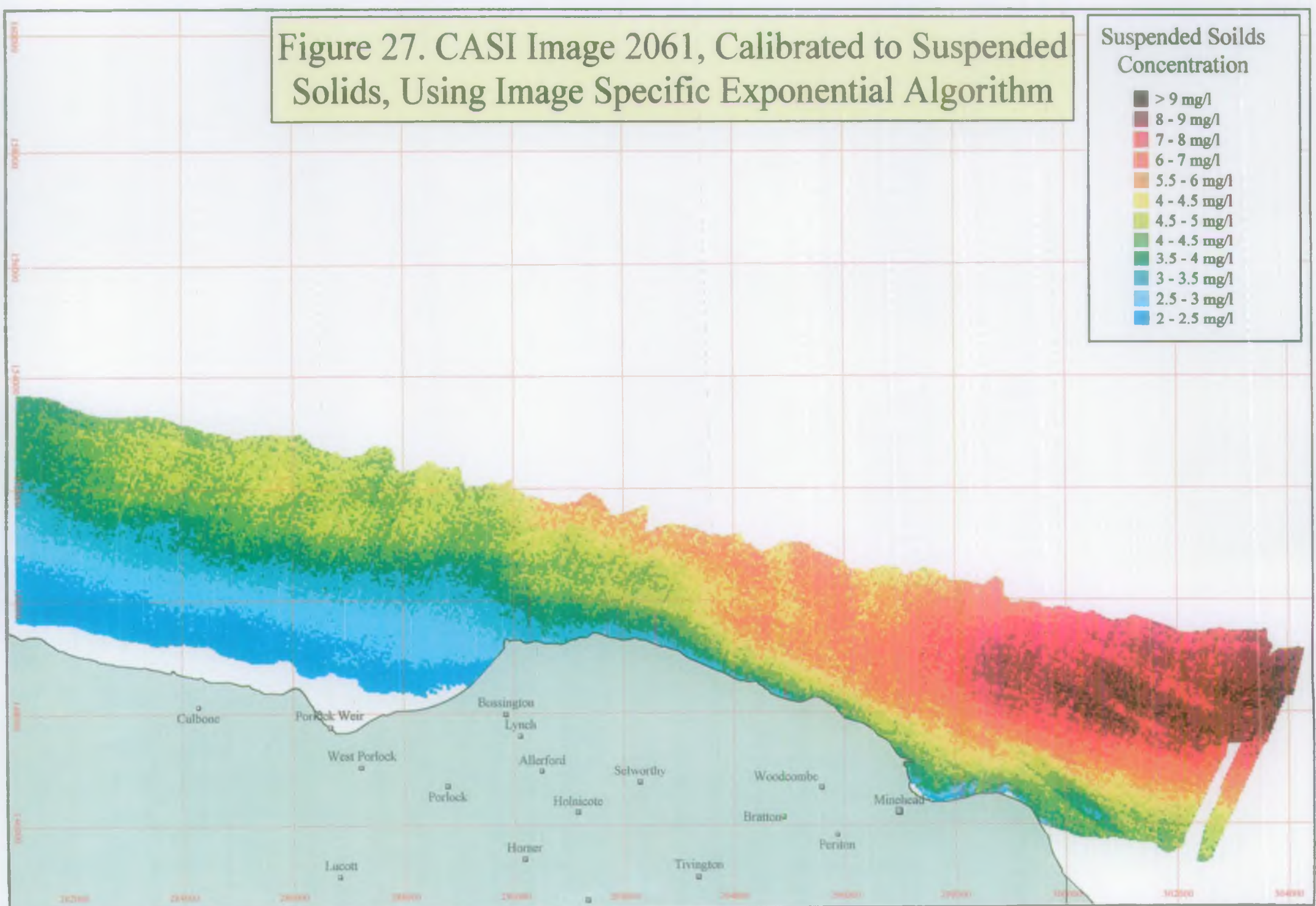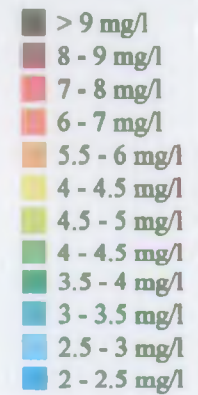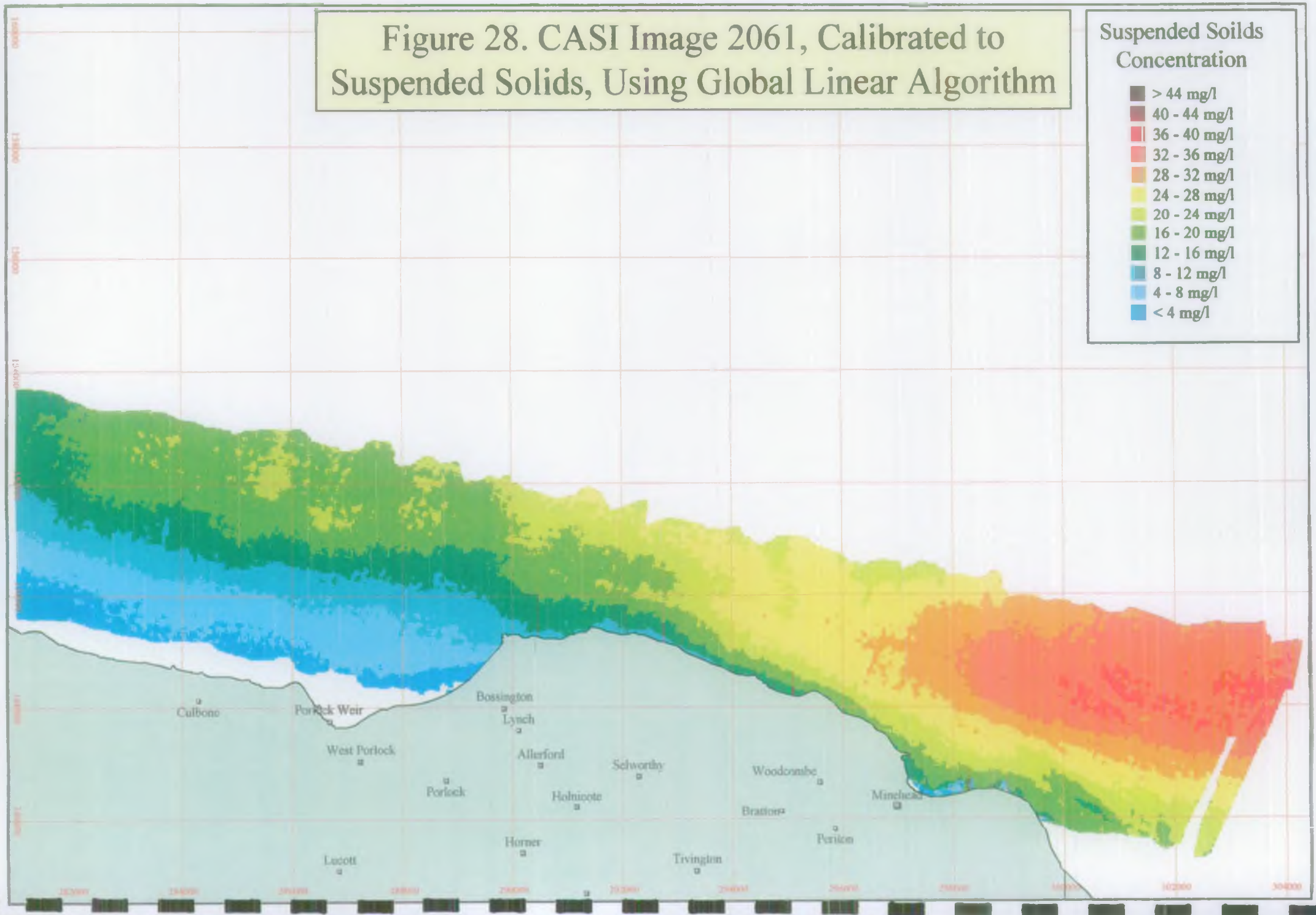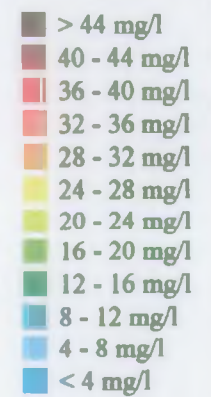- 3.5 - 4 mg/l
- 3 - 3.5 mg/l
- 2.5 - 3 mg/l
- 2 - 2.5 mg/l

Figure 28. CASI Image 2061, Calibrated to Suspended Solids, Using Global Linear Algorithm
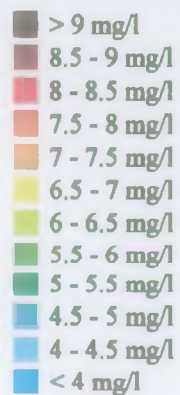
Suspended Soilds Concentration

- > 44 mg/l
- 40 - 44 mg/l
- 36 - 40 mg/l
- 32 - 36 mg/l
- 28 - 32 mg/l
- 24 - 28 mg/l
- 20 - 24 mg/l
- 16 - 20 mg/l
- 12 - 16 mg/l
- 8 - 12 mg/l
- 4 - 8 mg/l
- < 4 mg/l

Figure 29. CASI Images 2425 and 2426, Calibrated to Suspended Solids, Using Local (Bristol Channel) Linear Algorithm

Suspended Soilds Concentration

- > 9 mg/l
- 8.5 - 9 mg/l
- 8 - 8.5 mg/l
- 7.5 - 8 mg/l
- 7 - 7.5 mg/l
- 6.5 - 7 mg/l
- 6 - 6.5 mg/l
- 5.5 - 6 mg/l
- 5 - 5.5 mg/l
- 4.5 - 5 mg/l
- 4 - 4.5 mg/l
- < 4 mg/l
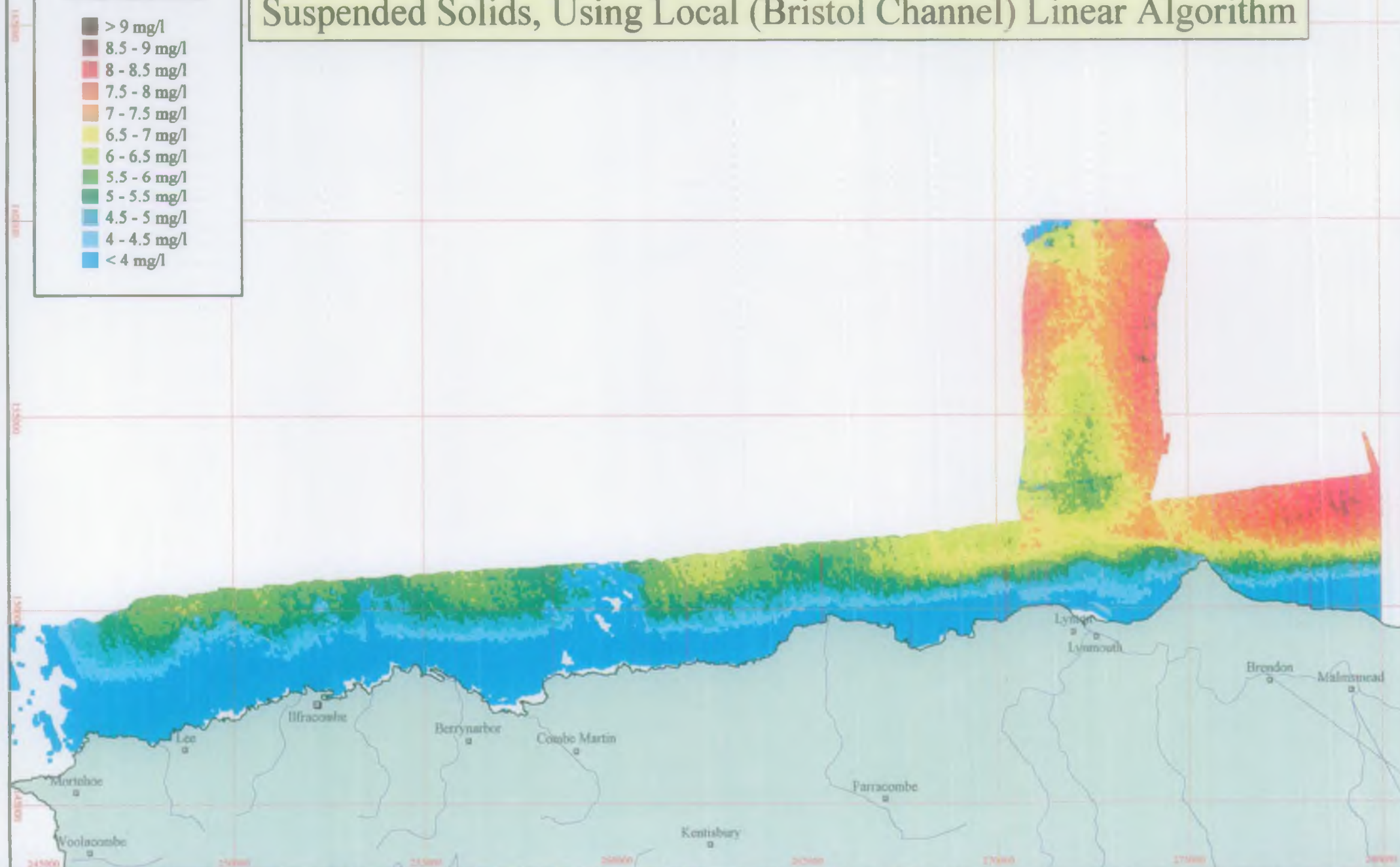
Figure 30. CASI Image 1877, Calibrated to Suspended Solids, Using Local (Norfolk) Linear Algorithm

Suspended Soilds Concentration

- > 20 mg/l
- 18 - 20 mg/l
- 16 - 18 mg/l
- 14 - 16 mg/l
- 12 - 14 mg/l
- 10 - 12 mg/l
- 8 - 10 mg/l
- 6 - 8 mg/l
- 4 - 6 mg/l
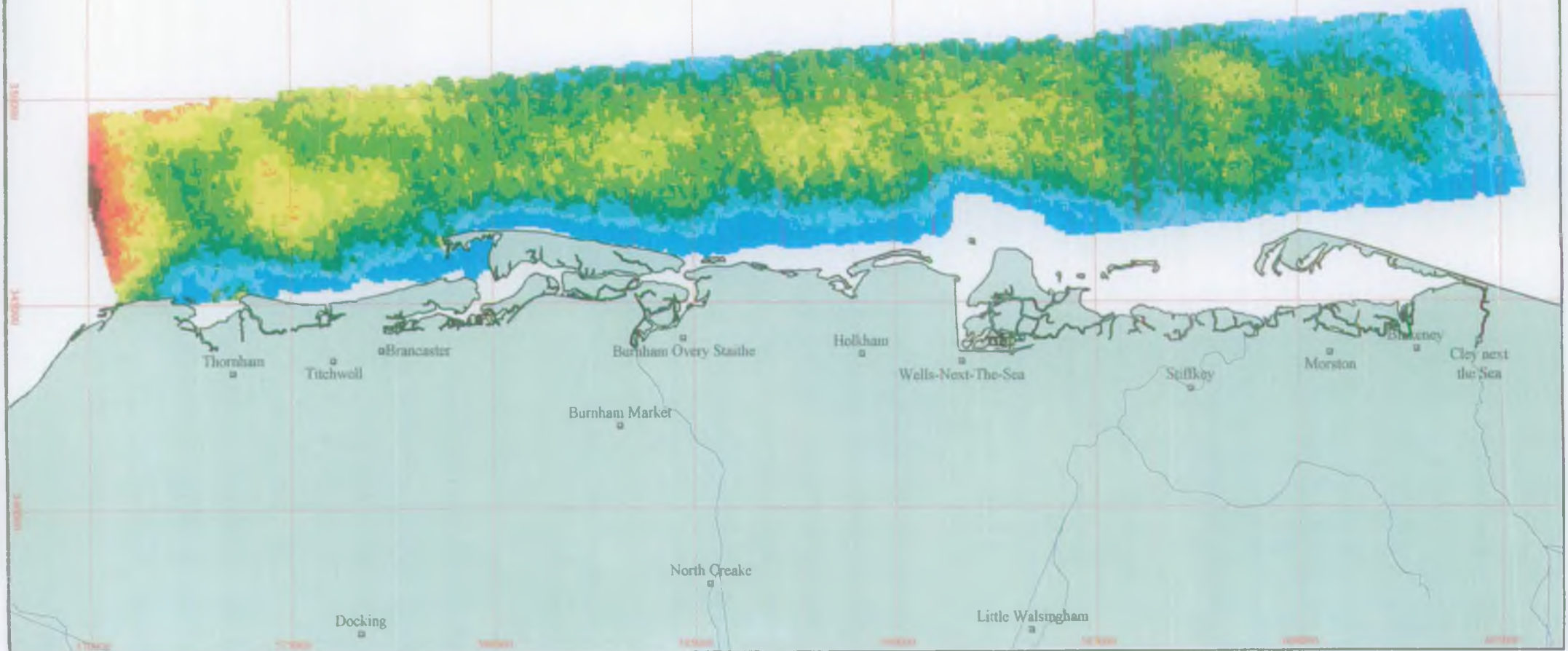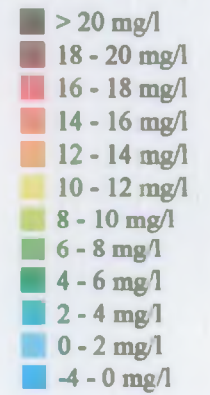- 2 - 4 mg/l
- 0 - 2 mg/l
- -4 - 0 mg/l

Figure 31. CASI Image 1875, 1876 and 1877 Calibrated to Suspended Solids, Using Image Specific (From Image 1875) Exponential Algorithm
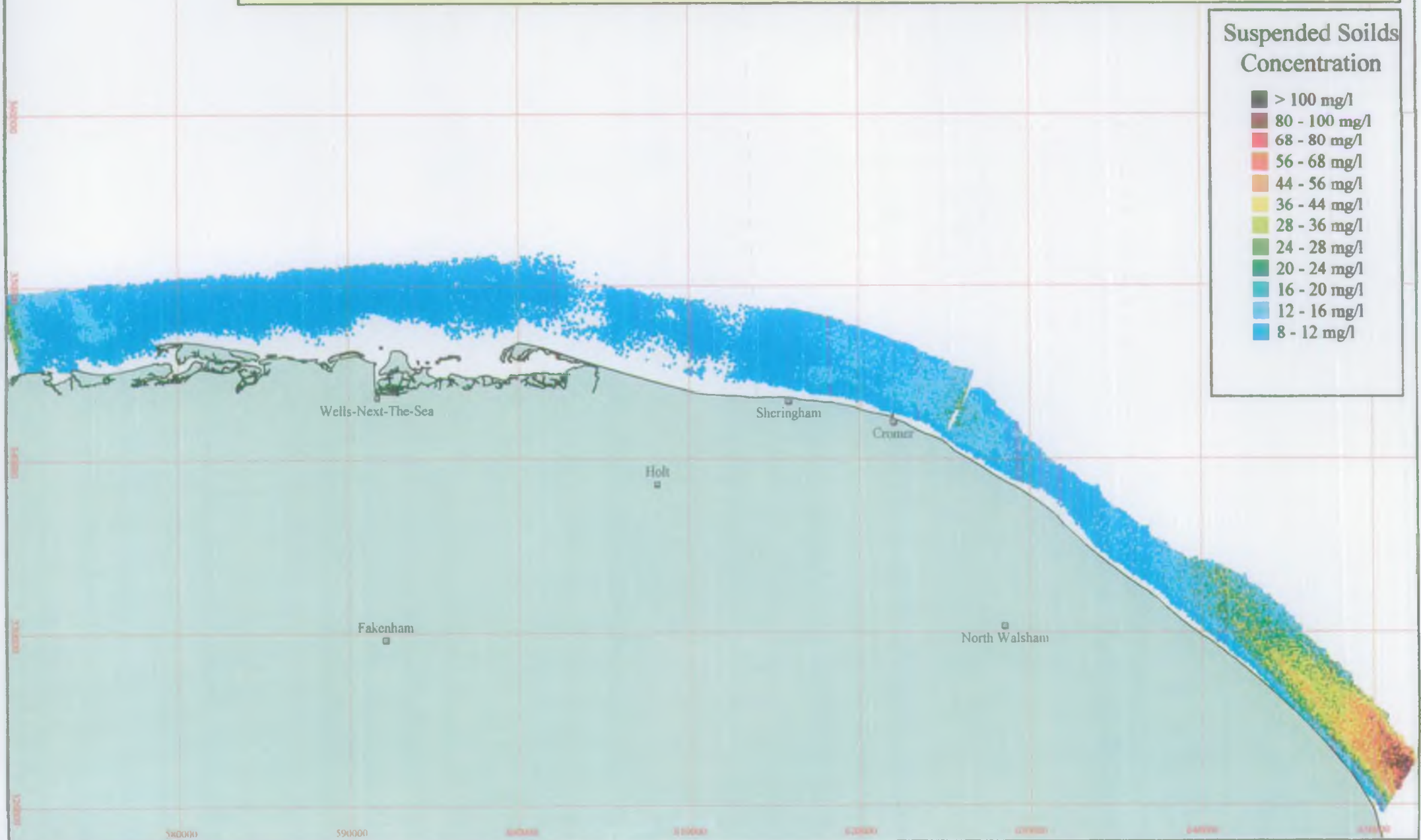
Figure 32. CASI Image 1877, Calibrated to Suspended Solids, Using Global Linear Algorithm

Suspended Soilds Concentration

- > 10 mg/l
- 9 - 10 mg/l
- 8 - 9 mg/l
- 7 - 8 mg/l
- 6 - 7 mg/l
- 5 - 6 mg/l
- 4 - 5 mg/l
- 3 - 4 mg/l
- 2 - 3 mg/l
- 1 - 2 mg/l
- 0 - 1 mg/l
- -2 - 0 mg/l